Xavier Domènech Figueras

TIME-CODED CHIPLESS RFID TAGS WITH CIRCULAR POLARIZATION

BACHELOR'S DEGREE FINAL PROJECT

Supervised by Prof. David Girbau Sala

Degree in Telematics Engineering

UNIVERSITAT ROVIRA I VIRGILI

Tarragona

2014

Acknowledgments:

To Dr. David Girbau, who helped me through all this project.

Index

1. Introduction

This project is about chipless RFID (Radio Frequency IDentification) tags, using Ultra-WideBand (UWB) technology and circular polarization. These tags will be time-coded and based on delay lines. This means that the tag consists of an ultra-wideband antenna connected to an open-ended delay line (see Figure 1.1).
The design of these antennas will be based on other authors' designs. The best antennas will be selected and re-designed to work on Rogers substrate and in the frequency band of the radar which will be used as reader. The delay lines will be integrated with these antennas and the resulting tags will be manufactured and tested.

1.1. RFID

RFID means Radio Frequency IDentification, and it is a wireless technology which uses radiofrequency signals to identify objects [3]. All this brings to mind bar codes, which have been widely used to identify the products we buy or official documentation. The features that makes RFID better than bar codes, are that RFID doesn't need direct view between the tag and the reader, tags are harder to damage, reprograming is allowed and the information it can contain is much bigger.
For a RFID communication there is a need of a reader and a tag. The reader will ask in a region (known as read range) for information of the tags scattered in this area. Then, the tags will answer and send its information to the reader.
There are two main types of tags: tags with chip or chipless tags. Tags with chip can be active if they are self-fed or passive if they use the power of the signal sent by the reader. On the other hand chipless tags are always passive, and these are the ones this project is about.

1.2. Chipless RFID

The research on chipless RFID tags is due to the fact that these tags are low-cost if we compare them to the tags with chip used for tagging applications which their cost is too high nowadays, even though it is expected that both types of tags have a similar cost than bar codes in future. In addition chipless tags might be future candidates to be used in harsh environments and as sensing modules of physical parameters.

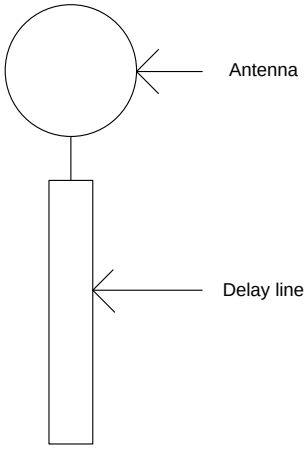

Figure 1.1. Structure of delay Line based tags.

Coding the information of a chipless RFID tag is not easy, but several solutions have been presented [2]. These solutions are classified in 3 main groups, as shown in Figure 1.2:

- Amplitude/Phase Backscatter modulations based.
- Special signature Based.
- TDR (Time-Domain Reflectometry) based.

This Project is based on TDR tags, and its subgroup Delay-Line-Based Tags. In order to read the tags, the radar Time Domain will be used, which is also a low-cost device.

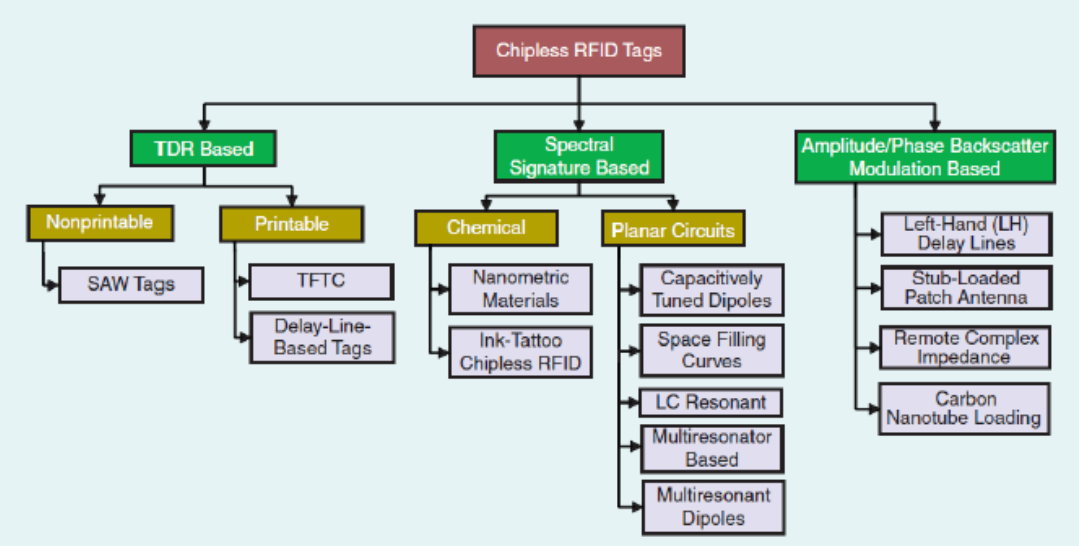

Figure 1.2. Classification of chipless RFID tags [2].

In delay-line-based tags, the response of the tag to an incoming signal from the reader contains two modes: a structural mode (the reflection of the wave at the structure of the tag) and the tag mode (the signal captured by the antenna that travels along the delay line and that is re-radiated). The tag mode contains the useful information that is the time delay between modes. The response of the tag to an incoming pulse (UWB signal) is shown in Figure 1.3.

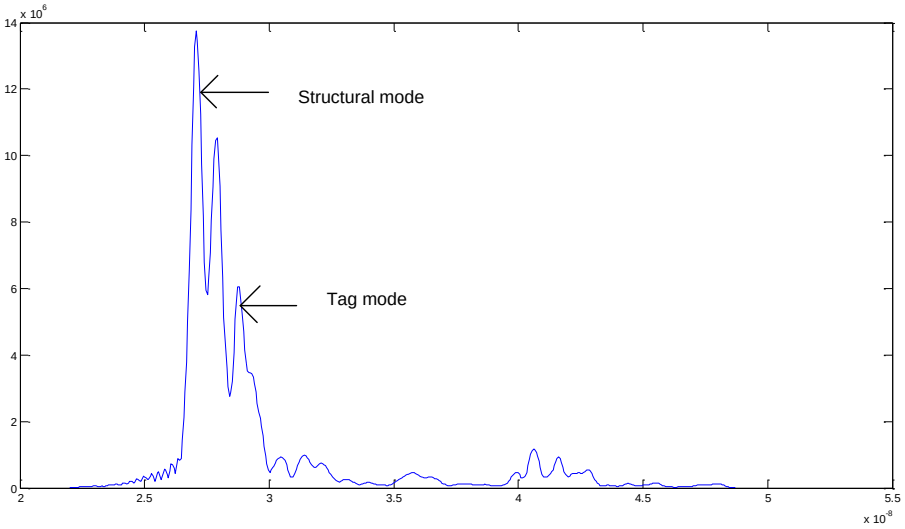

Figure 1.3. Structural and Tag mode in a chipless RFID tag.

1.3 Chipless RFID with Circular Polarization

The reader has two antennas, one for transmission and the other for reception, as shown in Figure 1.4. If the tag is linearly polarized the antennas will be placed in the same polarization and there will be a strong coupling between them, which can damage the lectures (read range reduction and impossibility of reading), but if the tag is circularly polarized, and linearly polarized antennas are used in the reader, one of the antennas of the reader can be rotated 90º, then the antennas would be cross-polarized and the coupling between them would be very low [1]. That's useful because as it was said before, chipless RFID tags use the power of the signal, which is received from de reader, and that means that the signal received by the reader will be very low, if the antennas are co-polarized, the coupling signal can be a problem and the data from the tag could be difficult to read, but if antennas are cross-polarized it would be much easier to read the tag. A tag circularly polarized can receive a signal polarized in one direction, and then send its own signal in both polarizations, which could be read by other antenna whatever the polarization it has. The problem is that there are no UWB tags which have a real circular polarization yet. There have been several researches in recent years on circularly-polarized antennas and work [1] proposes to integrate them in chipless tags, but there is no work showing experimental results of circularly-polarized chipless tags.

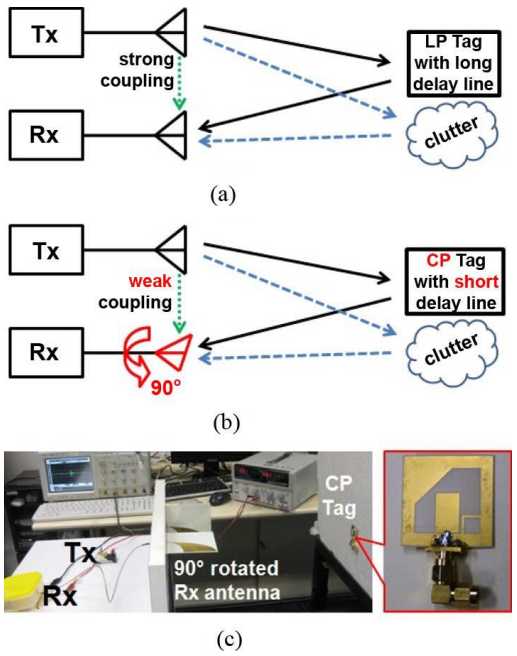

Figure 1.4. UWB-RFID systems using passive chipless tags [1].

1.4. Objectives

The principal aim of this project is to design a time-coded chipless RFID tag based on delay lines and with circular polarization. UWB antennas with circular polarization are complex to design and it will be a challenge to introduce them in real applications. Then, this is the main objective of this project. The other objectives of this project to accomplish it are the following:

- Collect and simulate UWB antennas with circular polarization designed by other authors.
- Replicate the UWB antennas chosen for evaluation and re-design them on Rogers RO4003 substrate.
- Integration of delay lines to UWB antennas with circular polarization.
- Measuring of circularly polarized UWB tags using an UWB radar.

1.5. Report Organization

This project is divided in 5 chapters:

- Chapter 2: antennas designed by other authors will be studied and simulated on ADS (Advance Design System) and the best antennas will be selected.
- Chapter 3: selected antennas will be optimized to work with Rogers substrate and in the frequency band of the radar. Also delay lines will be designed and integrated to the antennas.
-Chapter 4: RFID tags will be manufactured and measured with a UWB radar.
-Chapter 5: conclusions of the content of the project and suggestions of future lines.

References

[1] Yizhu Shen and Choi L. Law, "A Low-Cost UWB-RFID System Utilizing Compact Circularly Polarized Chipless Tags", "IEE ANTENNAS AND WIRELESS PROPAAGTION LETTERS, 2012, Vol. 11, pages 1382-1385.
[2] Stevan Preradovic and Nemai Chandra Karmakar. “Chipless RFID: Bar Code of the Future”, “IEE Microwave Magazine”, December 2010.
[3] Sergi Rima Martí, “Disseny d’antenes UWB per a optimització de tags chipless RFID”, Projecte de final de Carrera, Universitat Rovira i Virgili, 2011.

2. Literature Review of Circularly Polarized UWB Antennas

2.1. Introduction to UWB Antennas and Circular Polarization.

Since the aim of this chapter is to investigate and design UWB antennas with circular polarization, first there will be an introduction of the main concepts to be studied and then a research of some previously designed antennas by other authors. All the antennas will be simulated in ADS-Momentum (Advanced Design System).

2.1.1. UWB Antennas.

UWB antennas are used in technologies which demand a very large portion of the spectrum, usually more than 20% of the center frequency (BW > 20% of f_0), which means a small S_{11} along these frequencies. These antennas usually work at high frequencies (a few GHz). In Figure 2.1 the difference between an UWB antenna and a narrow-band (patch) antenna can be seen. Figure 2.1.a shows a very narrow bandwidth, it just works in a very specific frequency band. On the other hand, Figure 2.1.b has around 3 GHz of impedance matching bandwidth.

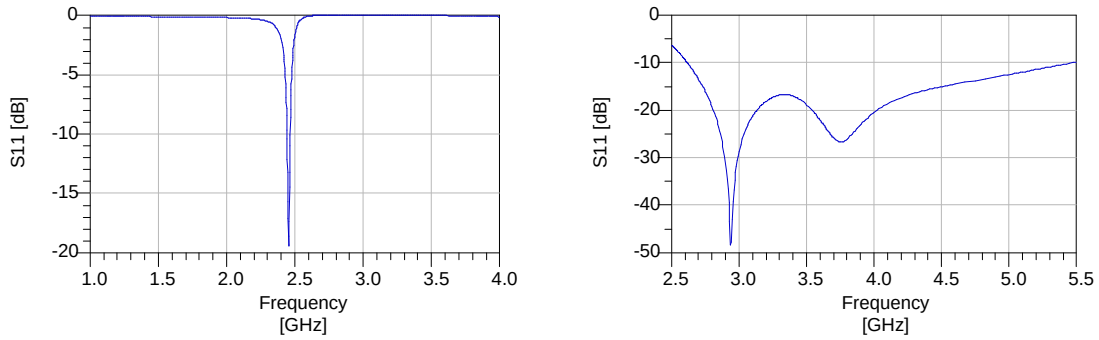

(a) Narrow band antenna **(b)** UWB antenna

Figure 2.1. Comparison between UWB antennas and narrow band antennas.

These UWB antennas are becoming more and more popular nowadays due to the fact, that their large bandwidth allow UWB systems to be implemented, which have a very low energy cost, a high data transfer rate, and strength against interferences and multipath effects. Nevertheless, the low energy levels that are used with these antennas also restricts their use to short range applications.

2.1.2 Circular Polarization.

Both the electric and magnetic fields are orthogonal and perpendicular to the wave's direction of travel. Polarization is defined by the extreme of the electric field vector and describes its movement; if it is in a single direction then it is called linear polarization but if it rotates with 0 dB between its maximum and minimum, then it is called circular polarization. The difference between maximum and minimum it is called Axial Ratio (AR), and this takes place when polarization is elliptical.

If an antenna is circularly polarized it enables to read signals coming from other antennas whatever its polarization is. It also enables to place the antenna in any direction to both receive and send data.
Many antennas with circular polarization have been designed and manufactured in a narrow band (less than 2%), and that's not enough for an UWB antenna. Other authors have tried different designs to enhance the Axial Ratio, some of these techniques are: embedding two inverted-L grounded strips around two opposite corners of the slot [8], embedding a T-shaped grounded metallic strip [4], embedding a spiral slot in the ground plane [9], or embedding a lightning-shaped feed line [7].

2.2. Design Specifications

The antennas will be tested using an UWB radar as reader. Figure 2.2 shows the short-pulses generated by a typical radar and the spectrum of three commercial radars can be observed in Fig. 2.3.

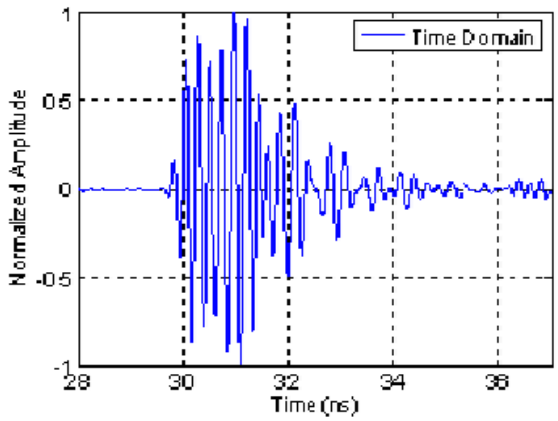

Figure 2.2 UWB Radar Pulse

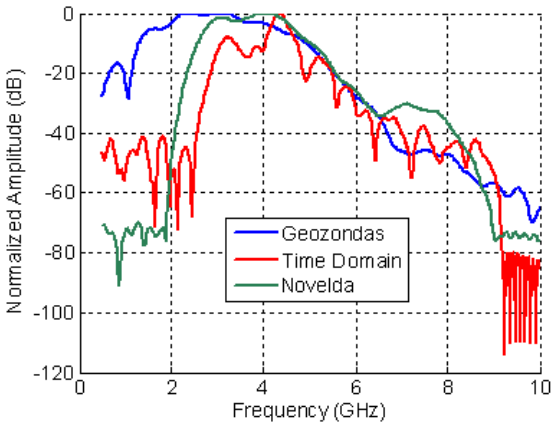

Figure 2.3 Power distribution of the Radar, the Radar which will be used is Time Domain

The radar used in this work is the Time Domain one. Then the bandwidth needed is (we consider power above -20 dB) approximately between 3 and 5 GHz with $f_o = 4.3\ GHz$, so antennas with a large bandwidth must be searched, preferably above 1 GHz.

Main parameters of the research will be return loss (S_{11}) and Axial Ratio, both of them should be as large as possible. S_{11} must be under -10 dB, and Axial Ratio below 3 dB. These parameters must have the bandwidth mentioned before (more than 1 GHz), but not necessarily be centered between 3 and 5 GHz in this chapter, since the selected designs will be optimized in next chapter. Also, as they will be RFID tags, they should be small antennas (antenna with the integrated delay line should not be bigger than a credit card).

2.3. UWB Antennas Circularly Polarized Research

2.3.1. Antenna [1]

The following antenna was designed in a coplanar waveguide feed structure, using a substrate of Rogers (RO4003C) with relative dielectric constant $\varepsilon_r = 3.38$, and thickness h = 0.508. The main design features are the grounded inverted-L strip and the truncated corner at the two opposite corners which help to realize circular polarization. Figure 2.4.a shows the layout of the original antenna and Fig. 2.4.b the layout that has been designed with ADS-Momentum. Fig. 2.5.a shows the simulated and measured S_{11} parameter in [1] and Figure 2.5.b shows the S_{11} simulated with ADS-Momentum. Fig. 2.6.a shows the simulated and measured axial ratio in [1] and Fig. 2.6.b shows the simulated axial ratio. Finally, Fig. 2.7 shows the simulated gain in [1] and the gain of the simulated design and Fig. 2.8 shows the 3D simulated radiation patterns for three frequencies.

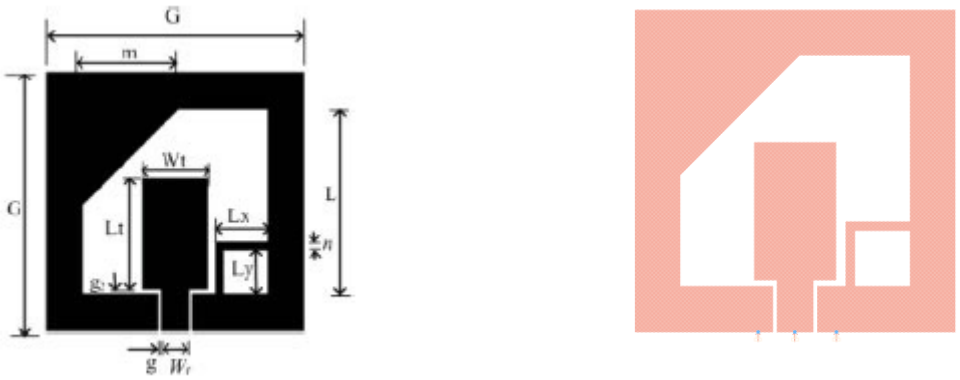

(a) Original Antenna. **(b)** Replicated Antenna.

Figure 2.4. Layouts of both original and replicated antennas.

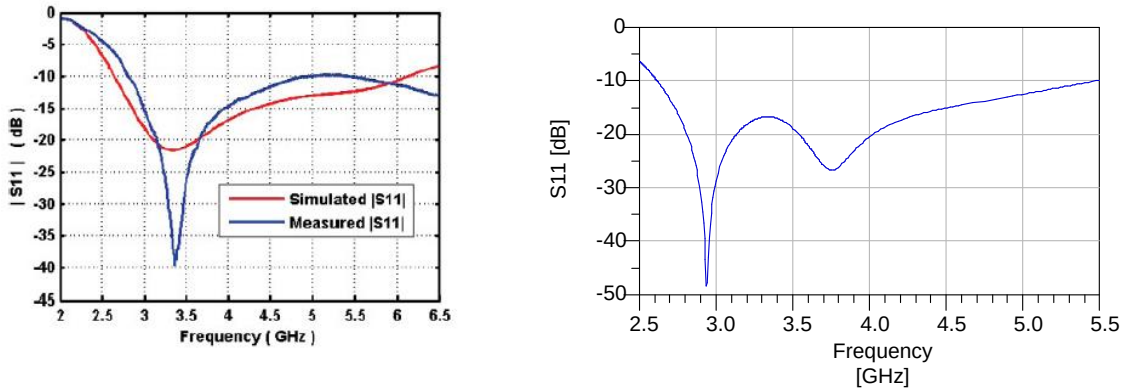

(a) Original antenna. **(b)** Replicated antenna.

Figure 2.5. Return loss of both original and replicated antennas.

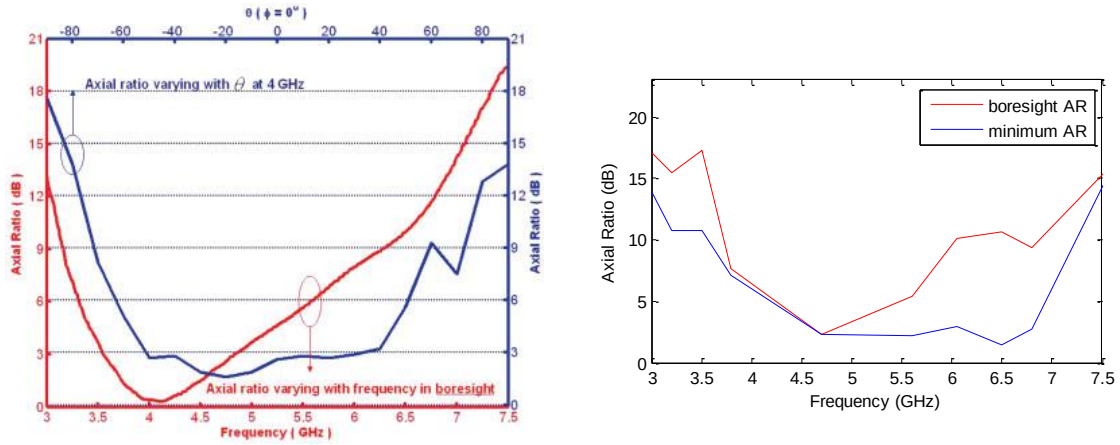

(a) Original antenna. **(b)** Replicated antenna.

Figure 2.6. Axial Ratio of both original and replicated antennas.

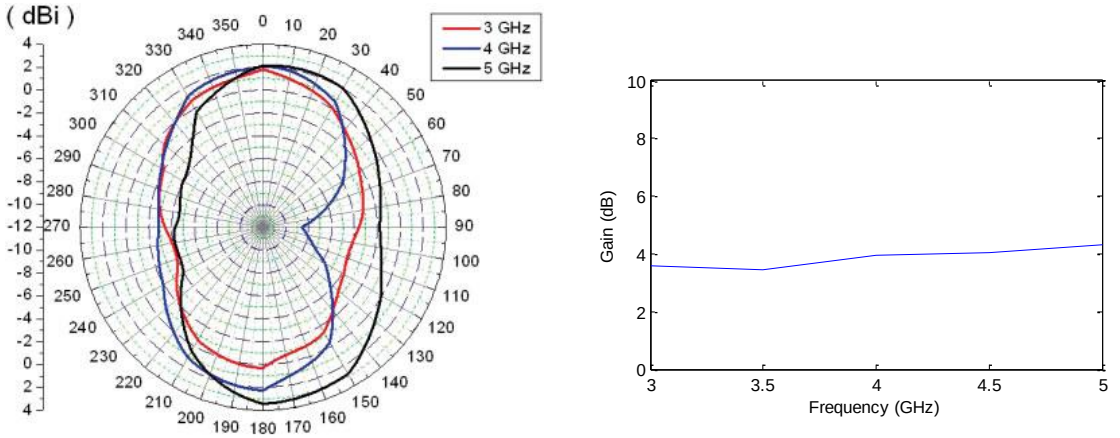

(a) Original antenna. **(b)** Replicated antenna.

Figure 2.7. Gain of both original and replicated antennas.

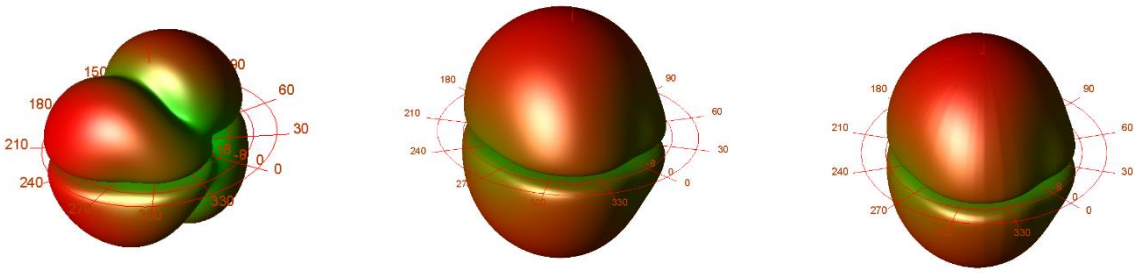

(a) 3 GHz. **(b)** 4 GHz. **(c)** 5 GHz.

Figure 2.8. Radiation Patterns of the replicated antenna in different frequencies.

2.3.2. Antenna [2]

This antenna was designed in a microstrip structure, an FR4 substrate (with relative dielectric constant $\varepsilon_r = 4.4$, and thickness $h = 1.6$ mm.) was used. The circular polarization is achieved by using an L-shaped strip with a taper end connected to a microstrip-line-fed. Other characteristic feature in this antenna is the circular-slot etched directly opposite of the L-shaped strip with the taper end in the ground plane. Figure 2.9.a shows the layout of the original antenna and Fig. 2.9.b the layout that has been designed with ADS-Momentum. Fig. 2.10.a shows the simulated and measured S_{11} parameter in [2] and Figure 2.10.b shows the S_{11} simulated with ADS-Momentum. Fig. 2.11.a shows the simulated and measured axial ratio in [2] and Fig. 2.11.b shows the simulated axial ratio. Finally, Fig. 2.12 shows the simulated gain in [2] and the gain of the simulated design and Fig. 2.13 shows the 3D simulated radiation patterns for four frequencies.

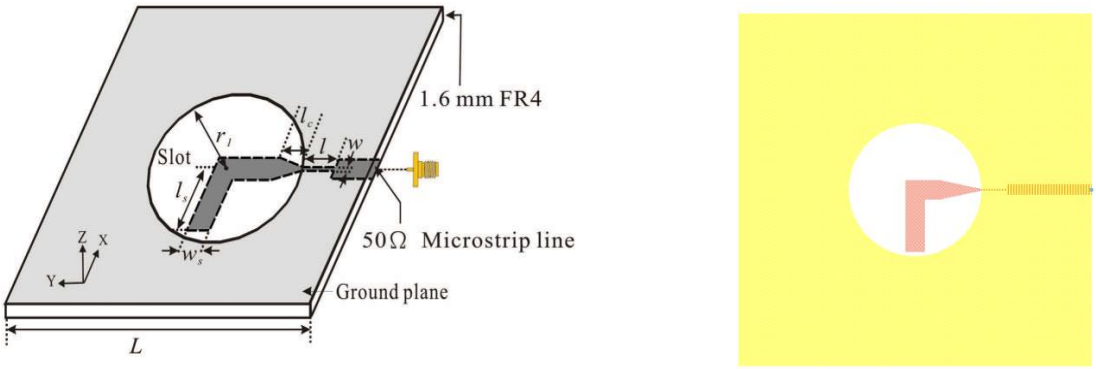

(a) Original Antenna. **(b)** Replicated Antenna.

Figure 2.9. Layouts of both original and replicated antennas.

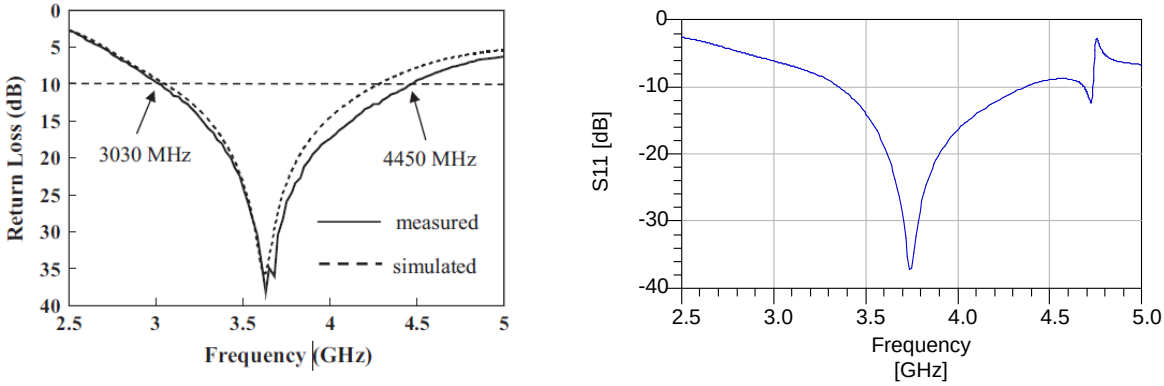

(a) Original antenna. **(b)** Replicated antenna.

Figure 2.10. Return loss of both original and replicated antennas.

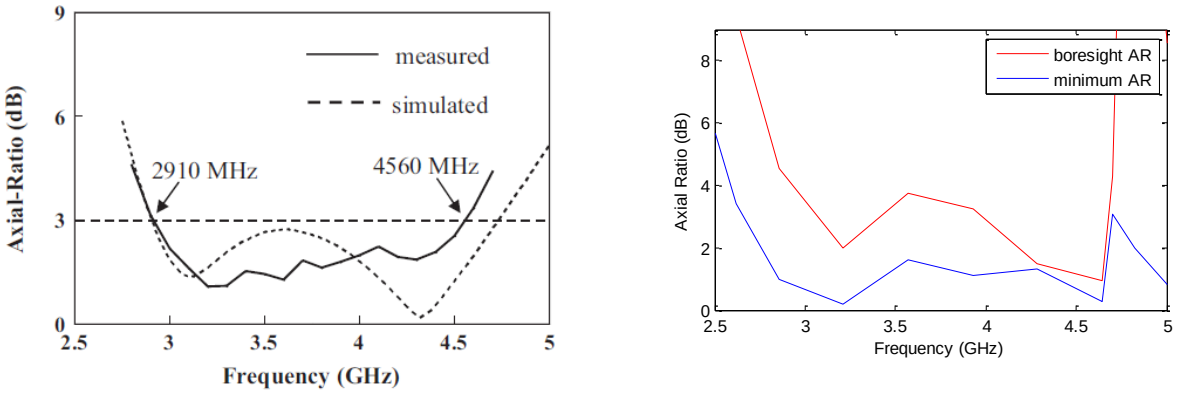

(a) Original antenna **(b)** Replicated antenna

Figure 2.11. Axial Ratio of both original and replicated antennas

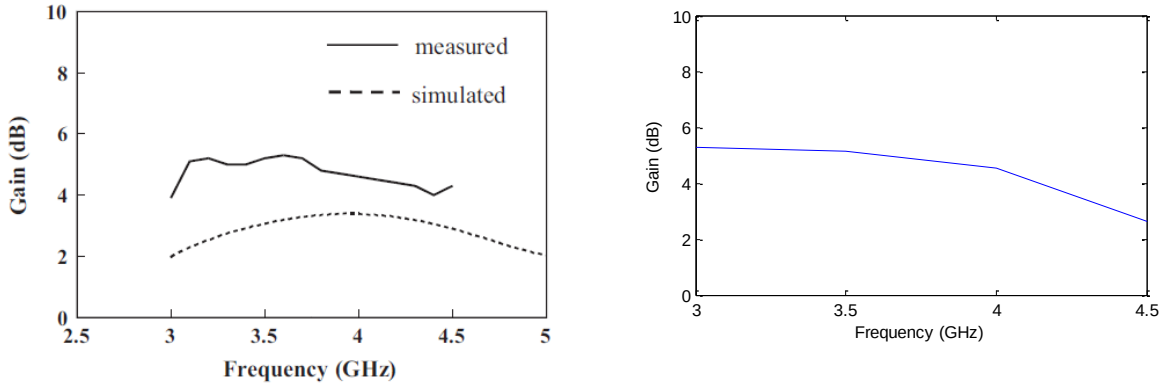

(a) Original antenna. **(b)** Replicated antenna.

Figure 2.12. Gain of both original and replicated antennas.

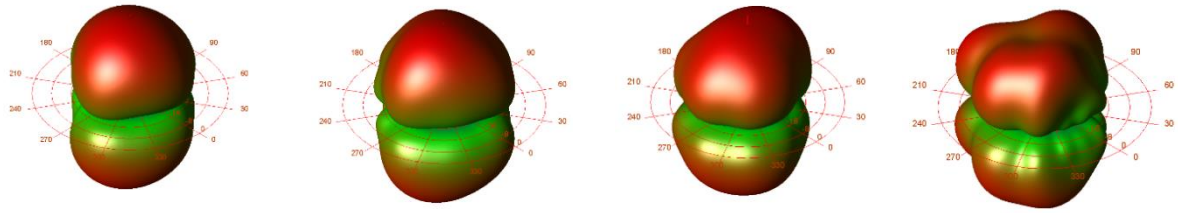

(a) 3 GHz. **(b)** 3.5 GHz. **(c)** 4 GHz. **(d)** 4.5 GHz.

Figure 2.13. Radiation Patterns of the replicated antenna at different frequencies.

2.3.3. Antenna [3]

This microstrip fed antenna was designed a FR4 substrate (thickness h = 1.6 mm, relative dielectric permittivity $\varepsilon_r = 4.2$ and tangent loss of 0.02). The antenna consists of a symmetric diamond shaped slot with a microstrip feed, optimizing this slot and the strip length, circularly polarized radiation can be achieved. Figure 2.14.a shows the layout of the original antenna and Fig. 2.14.b the layout that has been designed with ADS-Momentum. Fig. 2.15.a shows the simulated and measured S_{11} parameter in [3] and Figure 2.15.b shows the S_{11} simulated with ADS-Momentum. Fig. 2.16.a shows the simulated and measured axial ratio in [3] and Fig. 2.16.b shows the simulated axial ratio. Finally, Fig. 2.17 shows the simulated gain in [3] and the gain of the simulated design and Fig. 2.18 shows the 3D simulated radiation patterns for four frequencies.

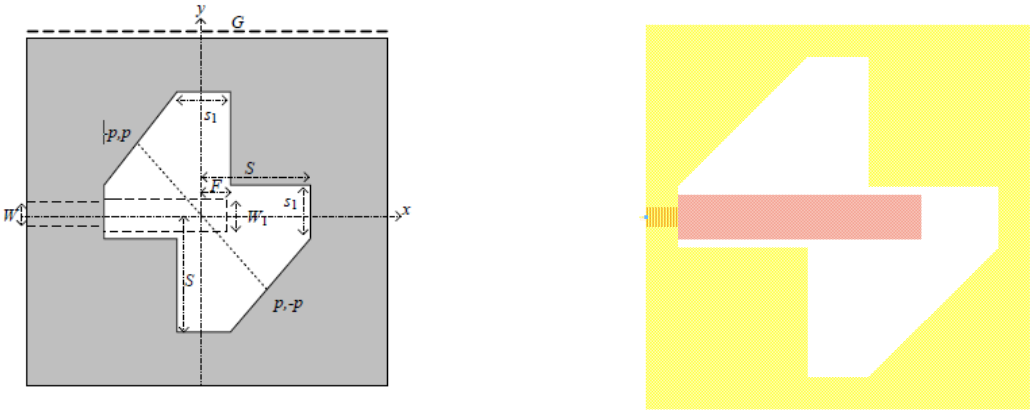

(a) Original Antenna. **(b)** Replicated Antenna.

Figure 2.14. Layouts of both original and replicated antennas.

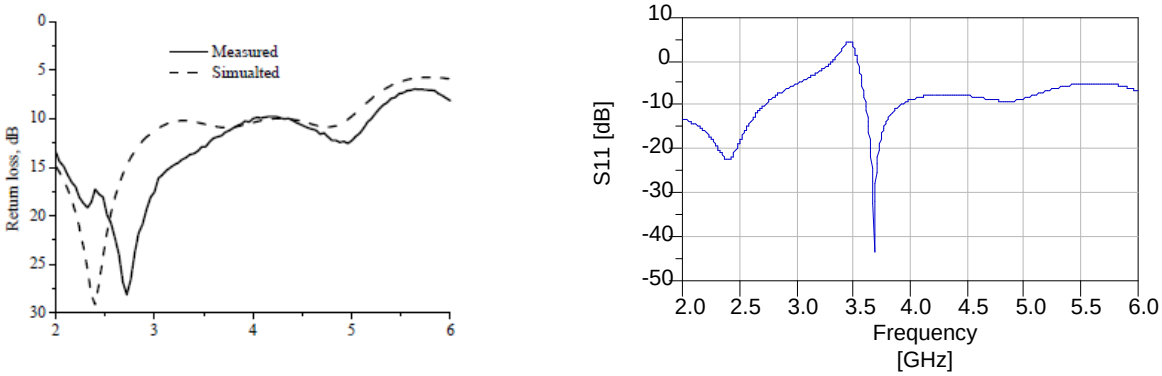

(a) Original antenna. **(b)** Replicated antenna.

Figure 2.15. Return loss of both original and replicated antennas.

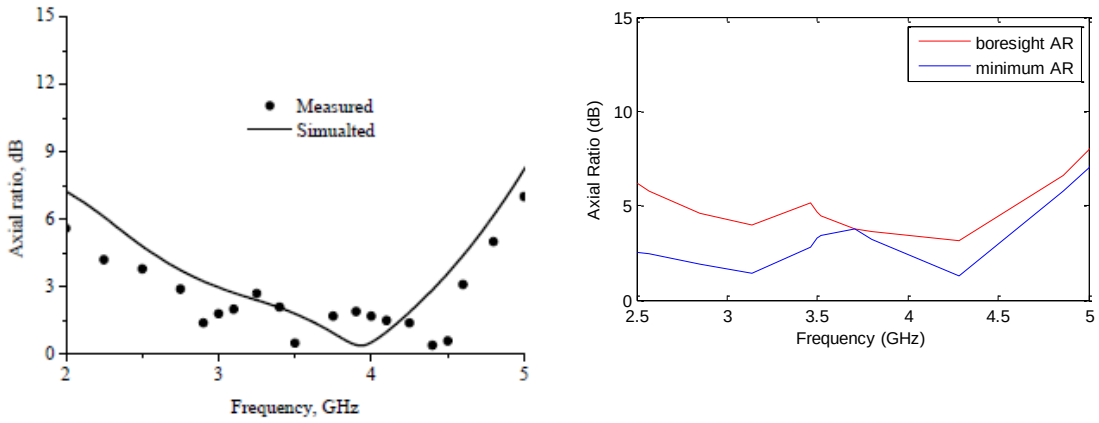

(a) Original antenna **(b)** Replicated antenna

Figure 216. Axial Ratio of both original and replicated antennas

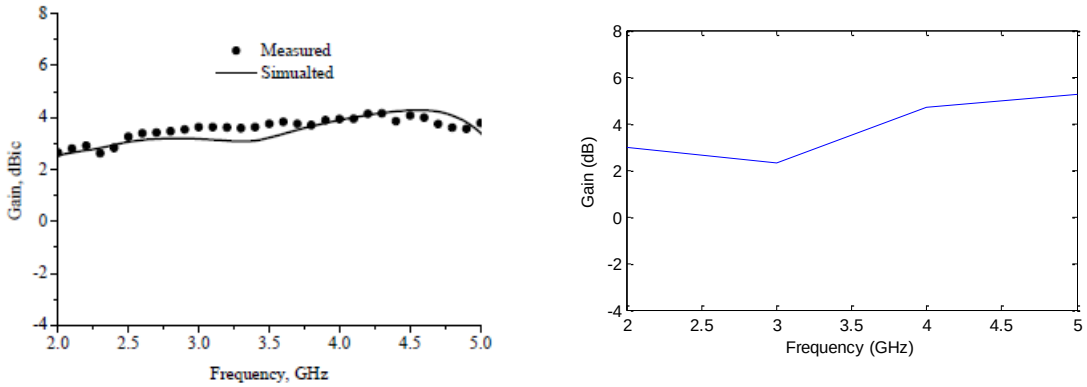

(a) Original antenna. **(b)** Replicated antenna.

Figure 2.17. Gain of both original and replicated antennas.

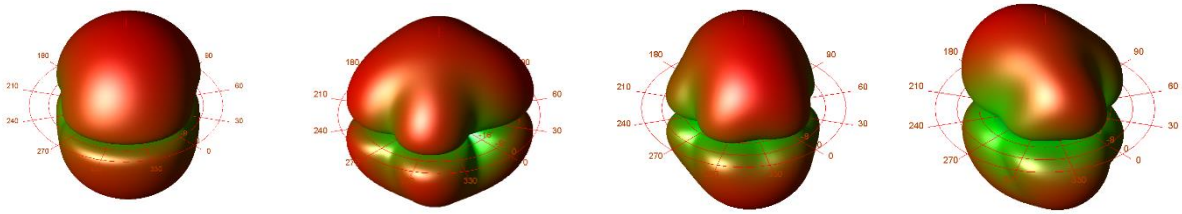

(a) 2 GHz. **(b)** 3 GHz. **(c)** 4 GHz. **(d)** 5 GHz.

Figure 2.18. Radiation Patterns of the replicated antenna at different frequencies.

2.3.4. Antenna [4]

This microstrip antenna was presented on a substrate with a relative permittivity $\varepsilon_r = 2.65$ and thickness h = 1 mm. The antenna is composed of a microstrip T-junction and a rectangular slot, with a T-shaped Stub on the conductor ground. The interaction of the T-shaped junction and the T-shaped stub increased the circular polarization bandwidth. Figure 2.19.a shows the layout of the original antenna and Fig. 2.19.b the layout that has been designed with ADS-Momentum. Fig. 2.20.a shows the simulated and measured S_{11} parameter in [4] and Figure 2.20.b shows the S_{11} simulated with ADS-Momentum. Fig. 2.21.a shows the simulated and measured axial ratio in [4] and Fig. 2.21.b shows the simulated axial ratio. Finally, Fig. 2.22 shows the simulated gain in [4] and the gain of the simulated design and Fig. 2.23 shows the 3D simulated radiation patterns for four frequencies.

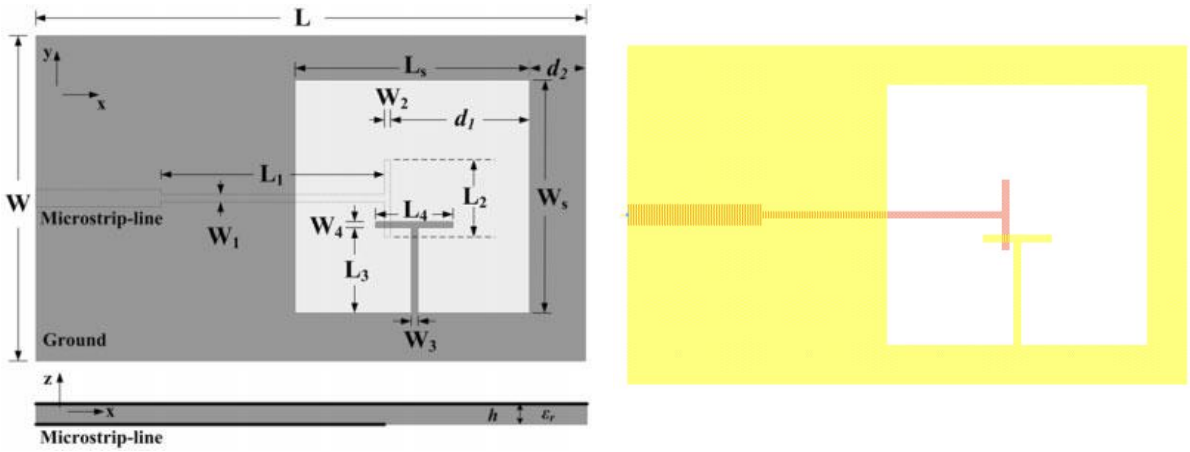

(a) Original Antenna. **(b)** Replicated Antenna.

Figure 2.19. Layouts of both original and replicated antennas.

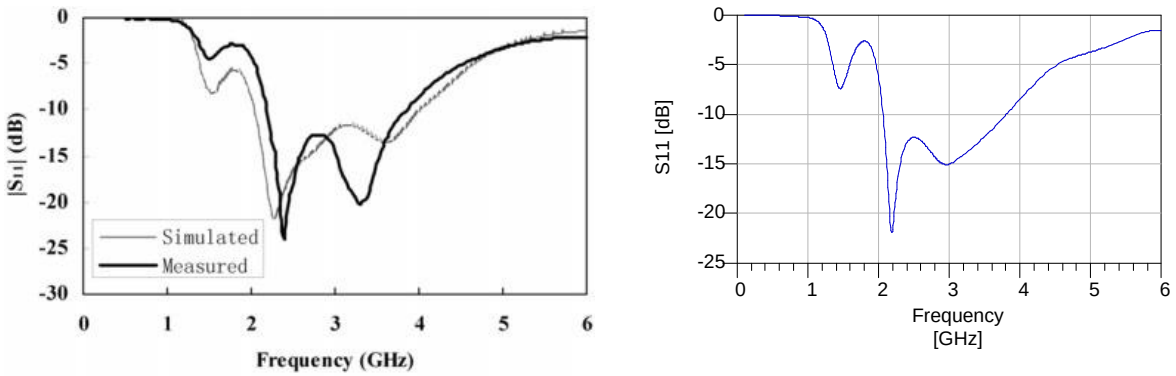

(a) Original antenna. **(b)** Replicated antenna.

Figure 2.20. Return loss of both original and replicated antennas.

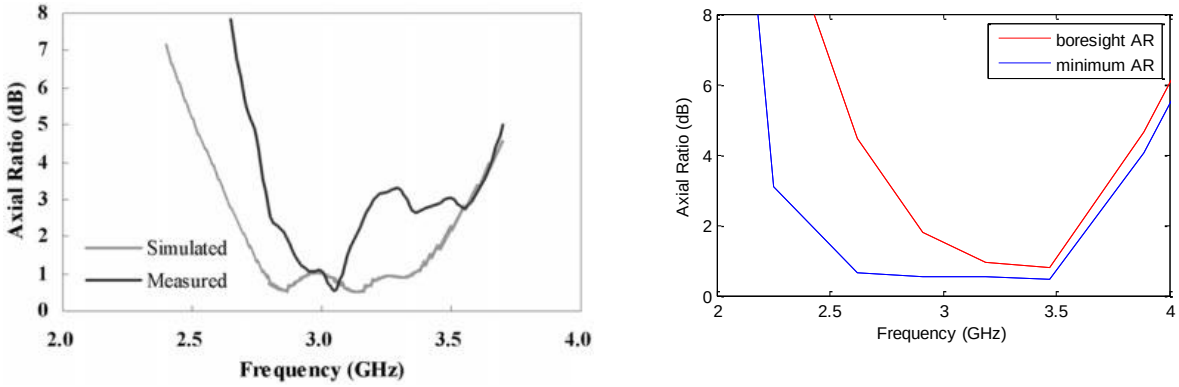

(a) Original antenna **(b)** Replicated antenna

Figure 2.21. Axial Ratio of both original and replicated antennas

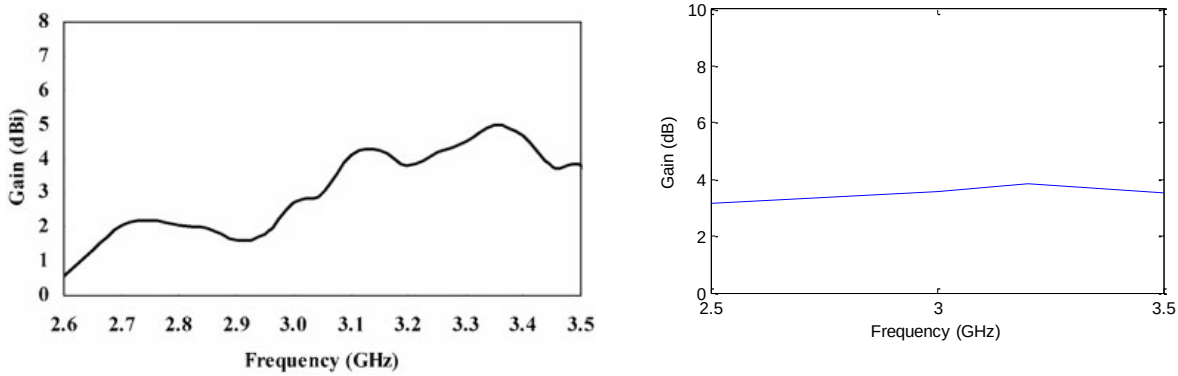

(a) Original antenna. **(b)** Replicated antenna.

Figure 2.22. Gain of both original and replicated antennas.

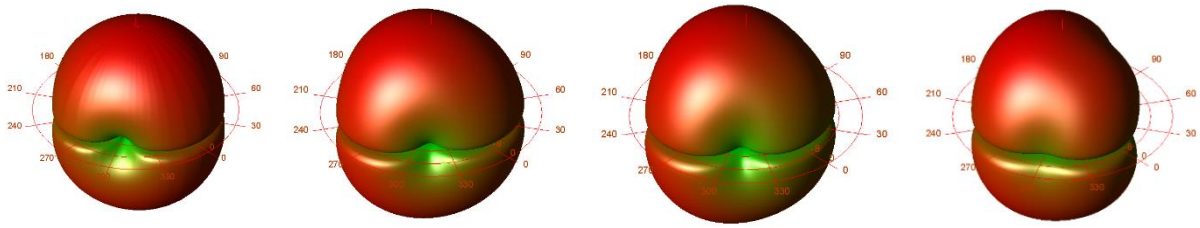

(a) 2 GHz. **(b)** 3 GHz. **(c)** 4 GHz. **(d)** 5 GHz.

Figure 2.23. Radiation Patterns of the replicated antenna at different frequencies.

2.3.5. Antenna [5]

This antenna was designed in a coplanar waveguide feed structure. A FR4 substrate was used with dielectric constant $\varepsilon_r = 4.3$, and thickness h = 1.53 mm. The main features are a fed transmission line extended into a trapezoidal shaped tuning stub located near the center of a rectangular slot and two grounded metallic arcs at two opposite corners of the slot. The grounded metallic arcs realize the circular polarization. Figure 2.24.a shows the layout of the original antenna and Fig. 2.24.b the layout that has been designed with ADS-Momentum. Fig. 2.25.a shows the simulated and measured S_{11} parameter in [5] and Figure 2.25.b shows the S_{11} simulated with ADS-Momentum. Fig. 2.26.a shows the simulated and measured axial ratio in [5] and Fig. 2.26.b shows the simulated axial ratio. Finally, Fig. 2.27 shows the simulated gain in [5] and the gain of the simulated design and Fig. 2.28 shows the 3D simulated radiation patterns for three frequencies.

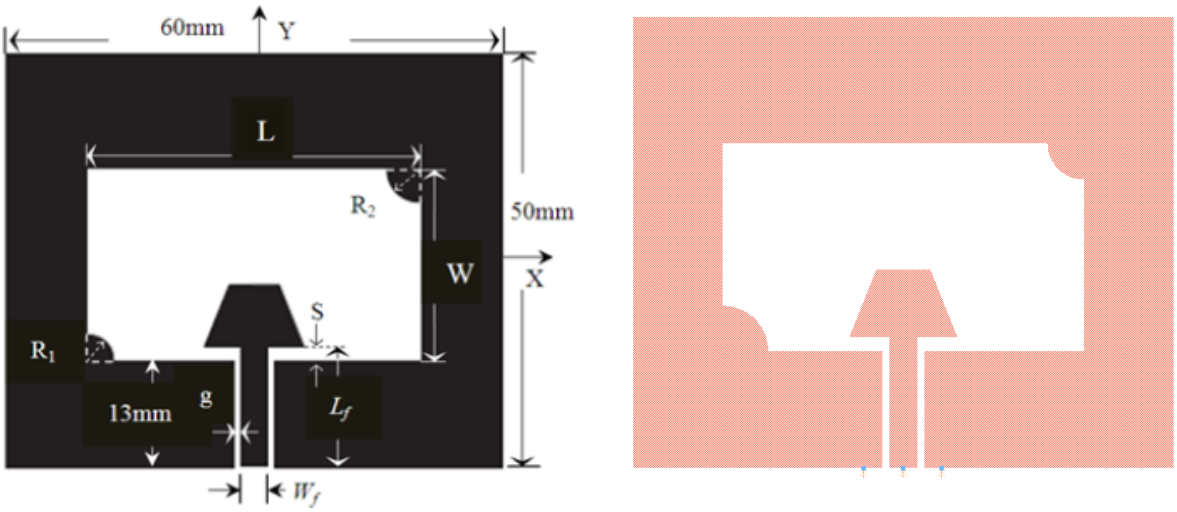

(a) Original Antenna. **(b)** Replicated Antenna.

Figure 2.24. Layouts of both original and replicated antennas.

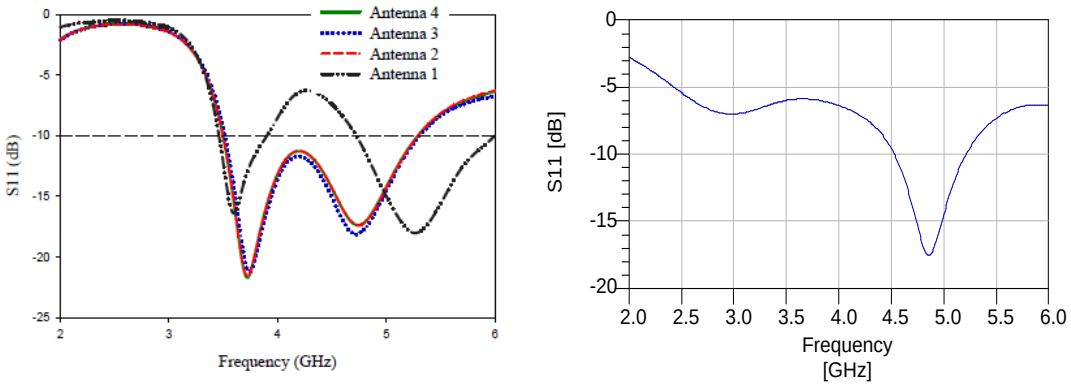

(a) Original antenna. **(b)** Replicated antenna.

Figure 2.25. Return loss of both original and replicated antennas.

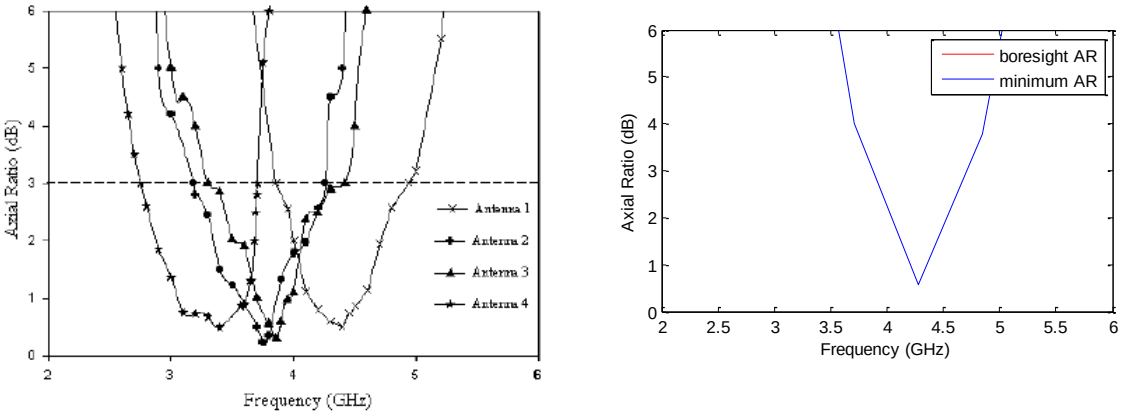

(a) Original antenna **(b)** Replicated antenna

Figure 2.26. Axial Ratio of both original and replicated antennas

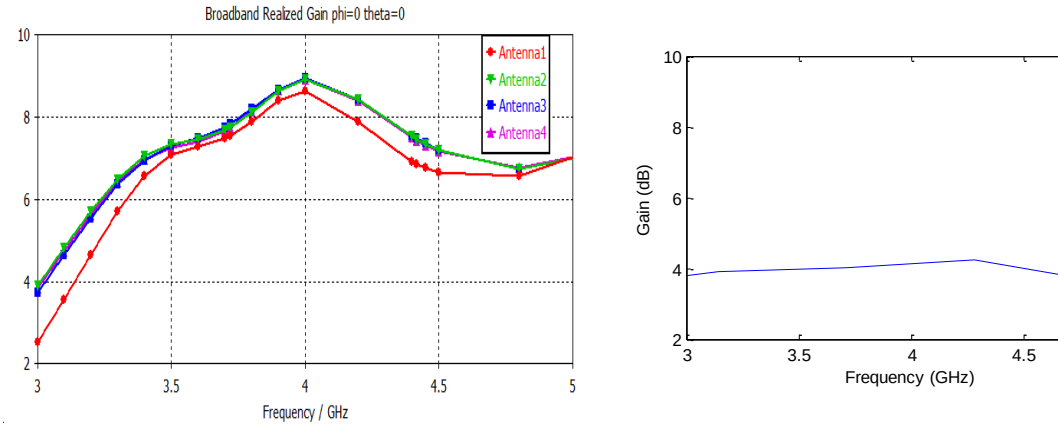

-a- Original antenna. **-b-** Replicated antenna.

Figure 2.27. Gain of both original and replicated antennas.

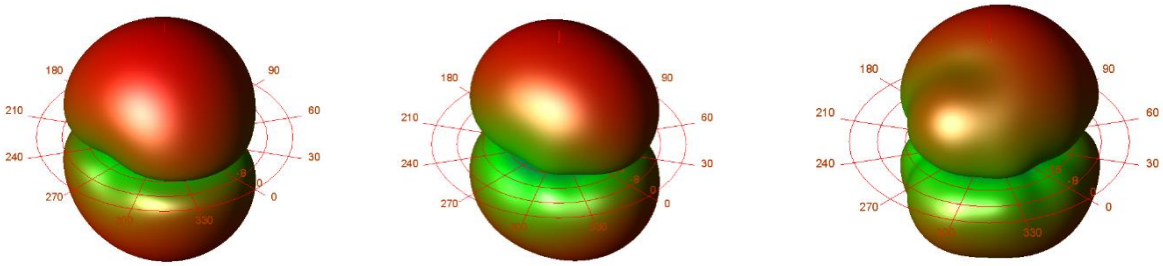

(a) 3 GHz. **(b)** 4 GHz. **(d)** 5 GHz.

Figure 2.28. Radiation Patterns of the replicated antenna at different frequencies.

2.3.6. Antenna [6]

The following CPW-fed antenna was designed using a FR-4 Substrate with the dielectric constant of 4.4, and thickness 0.9 mm. The structure of the antenna contains a stair-shaped slot on the ground plane with a longitudinal slot at the middle point of the first slot. The parameters of the longitudinal slot achieve the circular polarization. Figure 2.29.a shows the layout of the original antenna and Fig. 2.29.b the layout that has been designed with ADS-Momentum. Fig. 2.30.a shows the simulated and measured S_{11} parameter in [6] and Figure 2.30.b shows the S_{11} simulated with ADS-Momentum. Fig. 2.31.a shows the simulated and measured axial ratio in [6] and Fig. 2.31.b shows the simulated axial ratio. Finally, Fig. 2.32 shows the gain of the simulated design and Fig. 2.33 shows the 3D simulated radiation patterns for three frequencies.

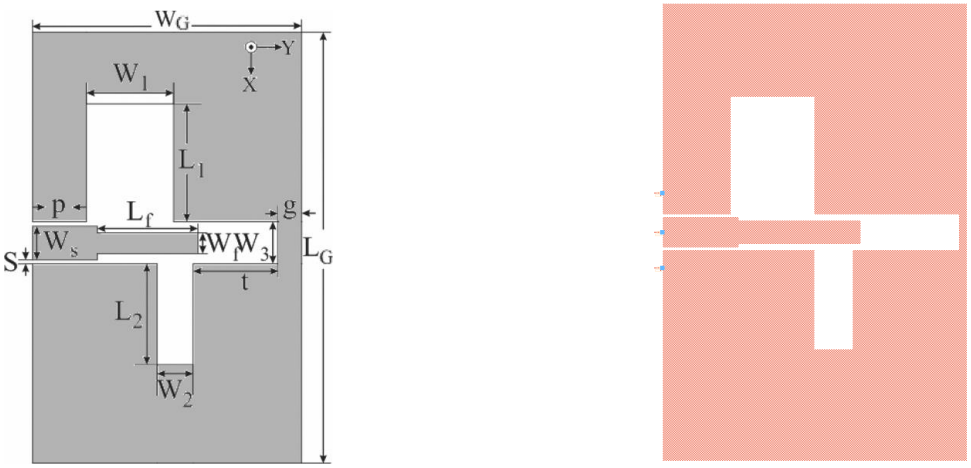

(a) Original Antenna. **(b)** Replicated Antenna.

Figure 2.29. Layouts of both original and replicated antennas.

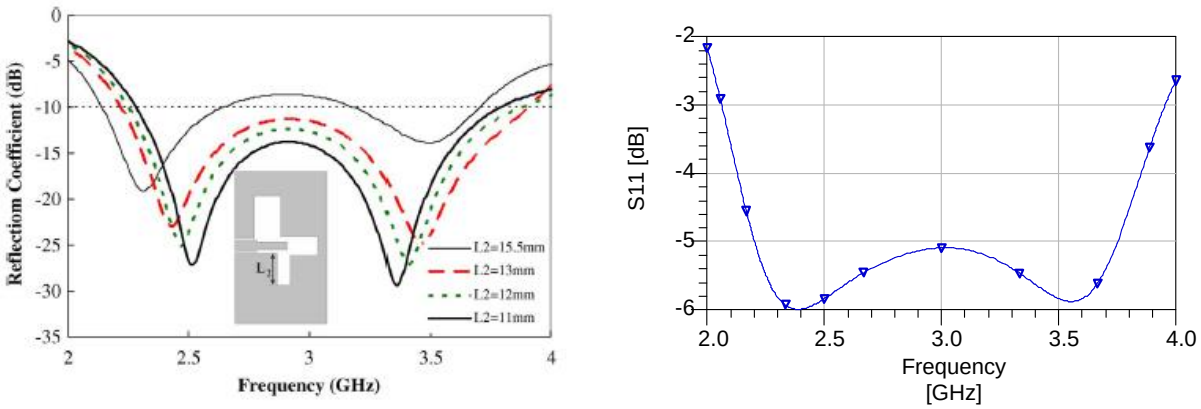

(a) Original antenna. **(b)** Replicated antenna.

Figure 2.30. Return loss of both original and replicated antennas.

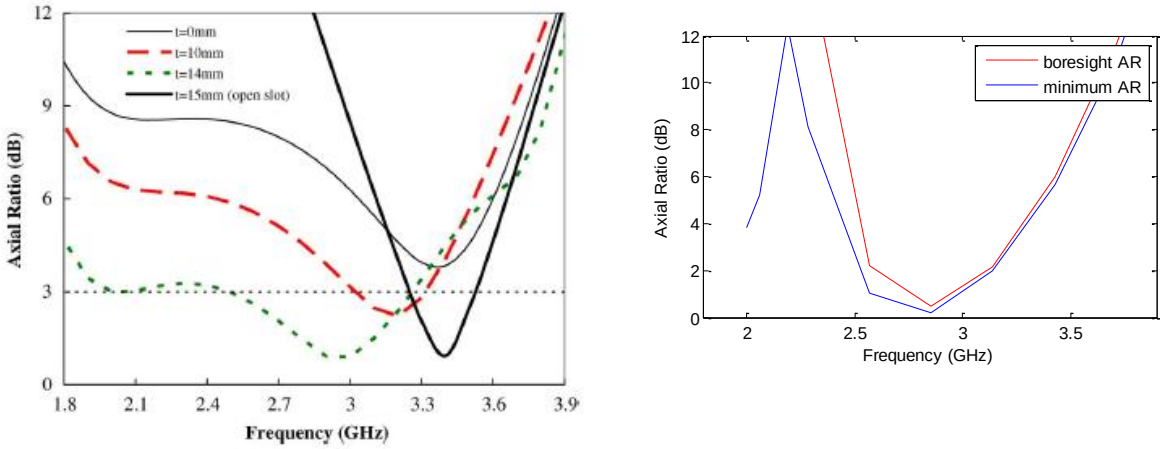

(a) Original antenna **(b)** Replicated antenna

Figure 2.31. Axial Ratio of both original and replicated antennas

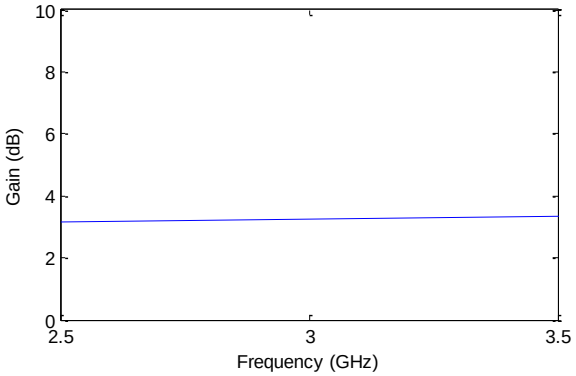

Figure 2.32. Gain of replicated antenna (gain of original antenna was not specified in the article).

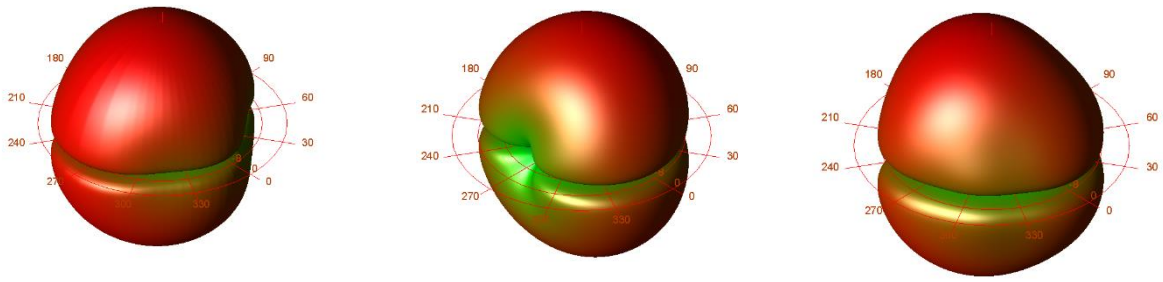

(a) 2 GHz. **(b)** **3** GHz. **(d)** 4 GHz.

Figure 2.33. Radiation Patterns of the replicated antenna at different frequencies.

2.3.7. Antenna [7]

This CPW antenna was printed on a substrate with dielectric constant $\varepsilon_r = 4.4$, tangent loss of 0.02 and thickness h = 0.8 mm. There are two main geometric features, the first one is the lightening-shaped feed line in conjunction with the two inverted-L grounded strips which helps to enhance the axial ratio, and the second one is the two tuning stubs in the feeding structure which realize the impedance matching. Figure 2.34.a shows the layout of the original antenna and Fig. 2.34.b the layout that has been designed with ADS-Momentum. Fig. 2.35.a shows the simulated and measured S_{11} parameter in [7] and Figure 2.35.b shows the S_{11} simulated with ADS-Momentum. Fig. 2.36.a shows the simulated and measured axial ratio in [7] and Fig. 2.36.b shows the simulated axial ratio. Finally, Fig. 2.37 shows the simulated gain in [7] and the gain of the simulated design and Fig. 2.38 shows the 3D simulated radiation patterns for three frequencies.

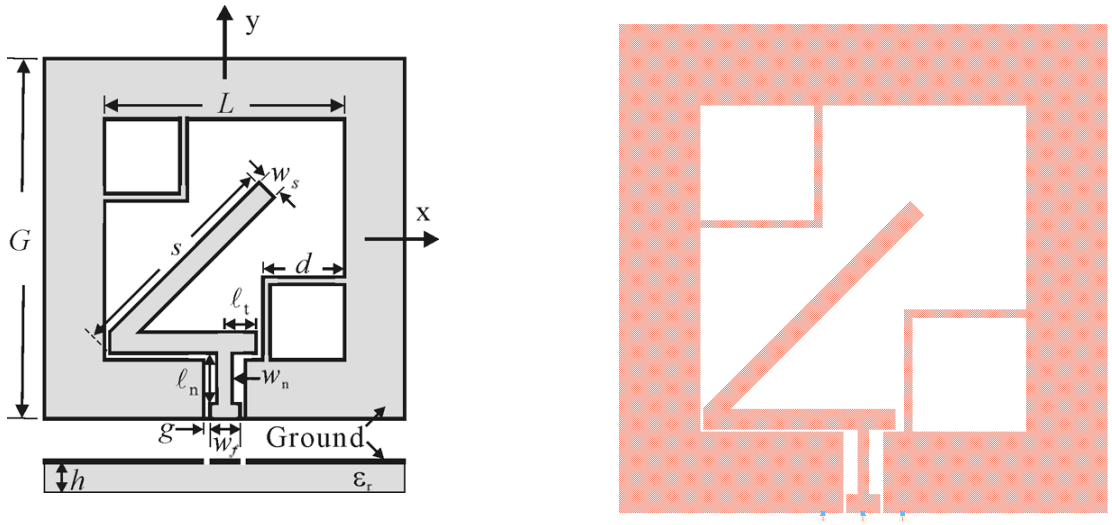

(a) Original Antenna. **(b)** Replicated Antenna.

Figure 2.34. Layouts of both original and replicated antennas.

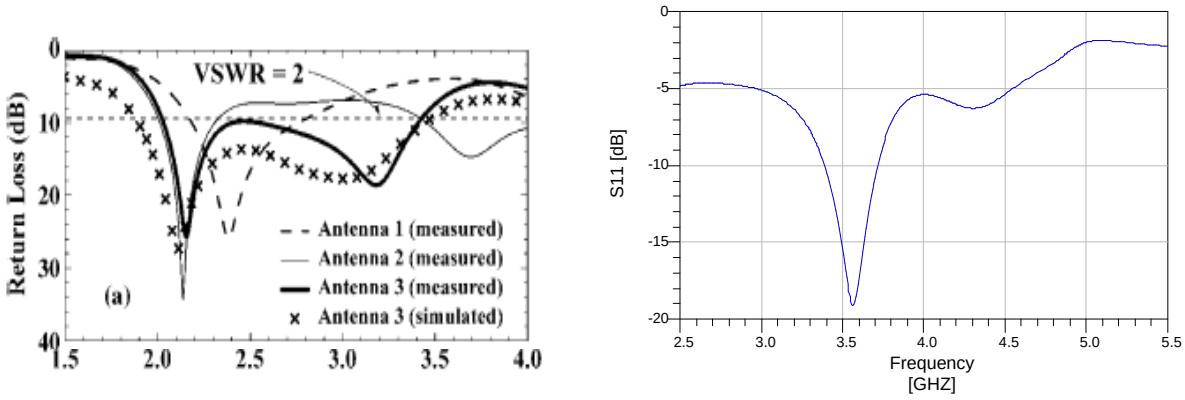

(a) Original antenna. **(b)** Replicated antenna.

Figure 2.35. Return loss of both original and replicated antennas.

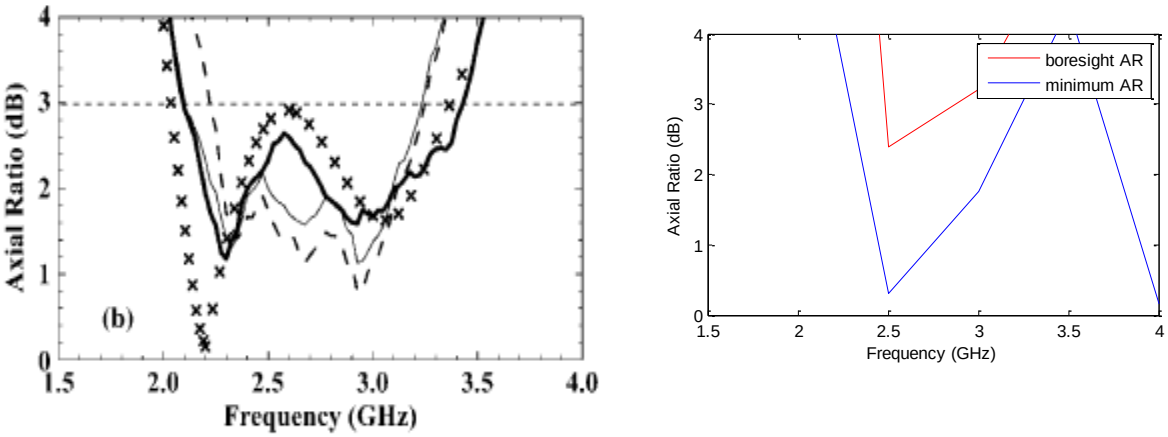

(a) Original antenna **(b)** Replicated antenna

Figure 2.36. Axial Ratio of both original and replicated antennas

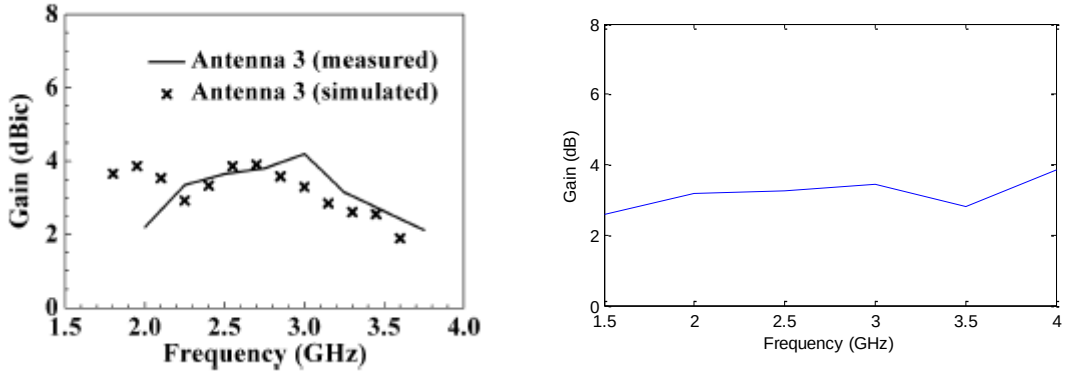

(a) Original antenna. **(b)** Replicated antenna.

Figure 2.37. Gain of both original and replicated antennas.

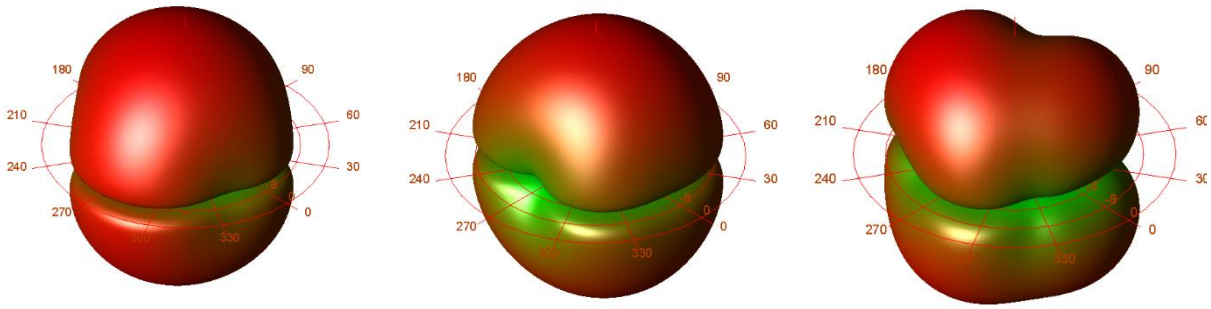

(a) 2 GHz. **(b)** **3** GHz. **(d)** 4 GHz.

Figure 2.38. Radiation Patterns of the replicated antenna at different frequencies.

2.3.8. Antenna [8]

This last antenna was printed in a CPW-fed structure using a FR-4 substrate with permittivity $\varepsilon_r = 4.4$, a loss tangent of 0.024 and thickness h= 0.8 mm. Impedance bandwidth was achieved by the two tuning stubs in the feeding structure, and axial ratio bandwidth was reached by the two unequal-size inverted-L strips placed around two opposite corners of the square slot. One parameter was not specified, so a few simulations were made by varying the gap between the down left square and the tuning stub with the slit. Figure 2.39.a shows the layout of the original antenna and Fig. 2.39.b the layout that has been designed with ADS-Momentum. Fig. 2.40.a shows the simulated and measured S_{11} parameter in [8] and Figure 2.40.b shows the S_{11} simulated with ADS-Momentum. Fig. 2.41.a shows the simulated and measured axial ratio in [8] and Fig. 2.41.b shows the simulated axial ratio. Finally, Fig. 2.42 shows the simulated gain in [8] and the gain of the simulated design and Fig. 2.43 shows the 3D simulated radiation patterns for four frequencies.

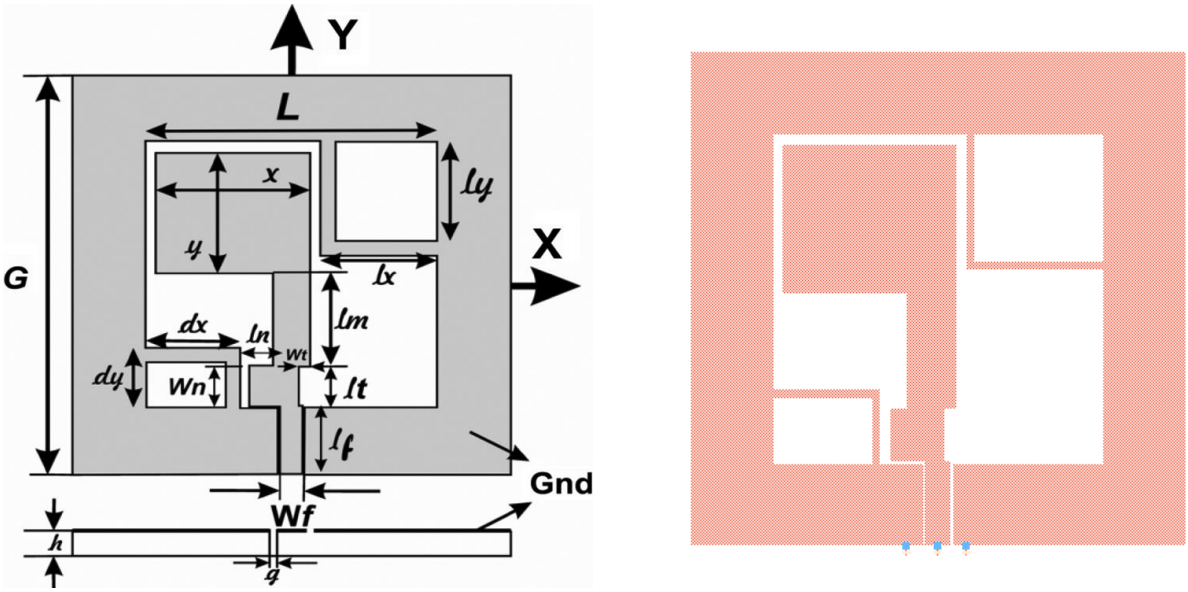

(a) Original Antenna. **(b)** Replicated Antenna.

Figure 2.39. Layouts of both original and replicated antennas.

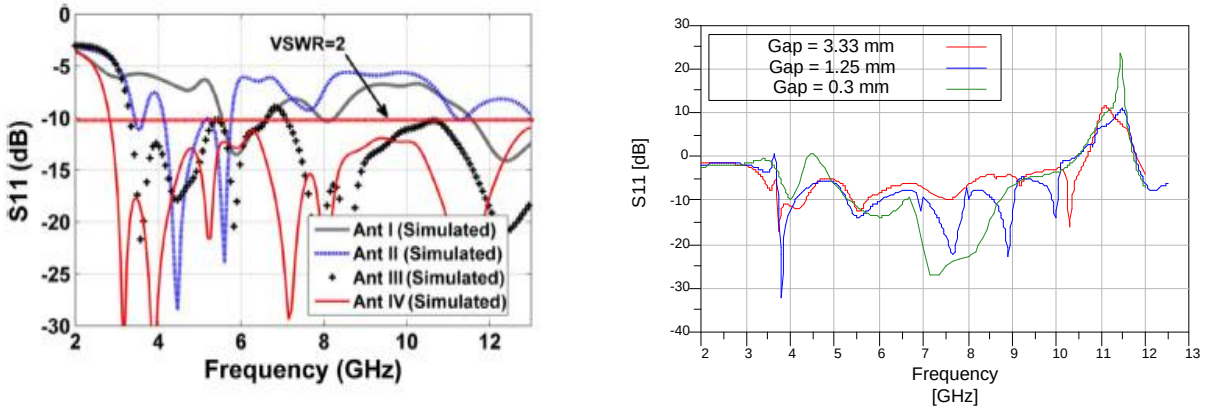

(a) Original antenna. **(b)** Replicated antenna.

Figure 2.40. Return loss of both original and replicated antennas.

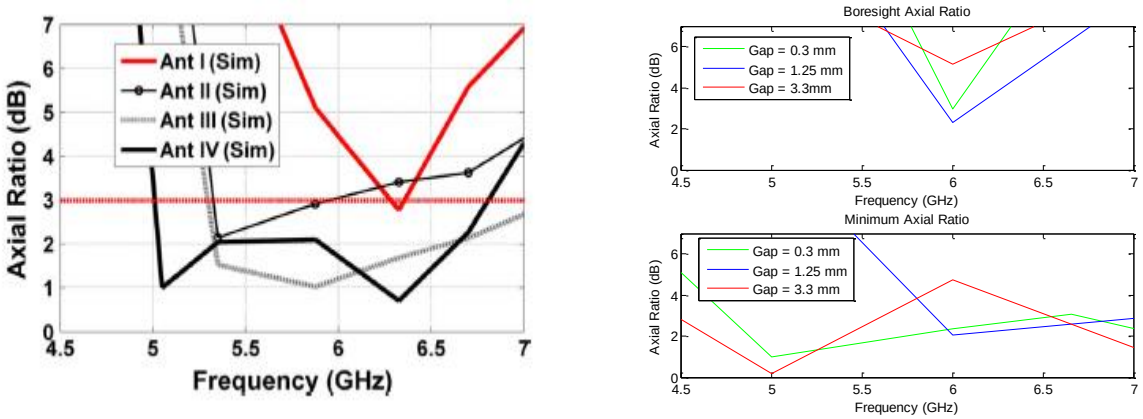

(a) Original antenna **(b)** Replicated antenna

Figure 2.41. Axial Ratio of both original and replicated antennas

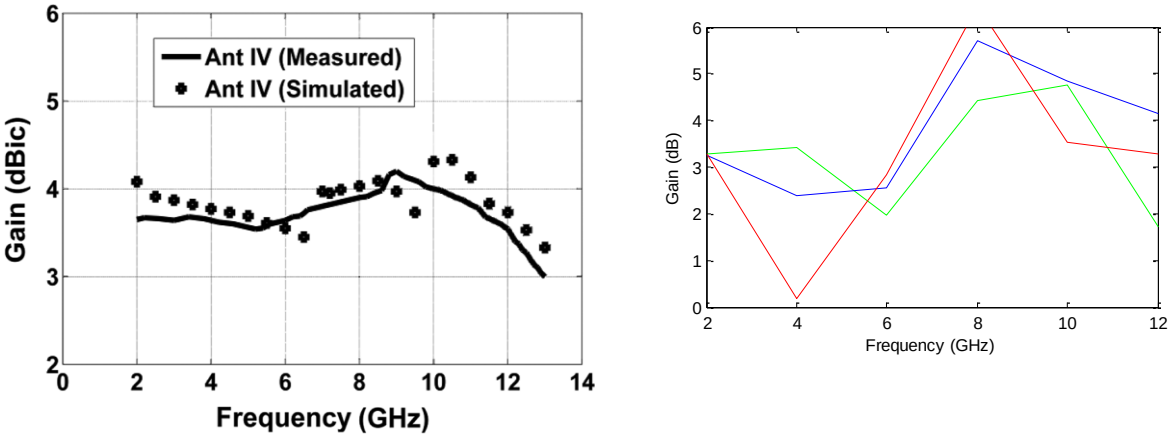

(a) Original antenna. **(b)** Replicated antenna.

Figure 2.42. Gain of both original and replicated antennas.

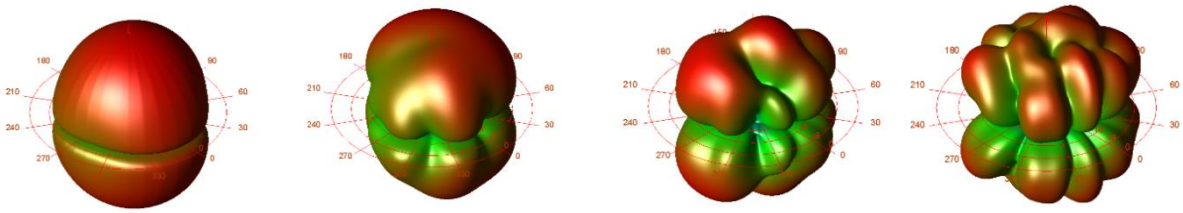

(a) 2 GHz. **(b)** 5 GHz. **(d)** 8 GHz. **(2)** 12 GHz.

Figure 2.43. Radiation Patterns of the replicated antenna at different frequencies with Gap = 1.25 mm.

2.4. Comparison and Conclusion of the Antennas.

Some antennas have been simulated, some of them with good results, some others with unexpected results. There was also an antenna [9], which couldn't be simulated due to complexity of its design, and there wasn't a way to draw it with the program which was used.

Antennas [3], [5], [6], [7] and [8], didn't work as expected. Antenna [3] didn't have same results as the original article, the reason couldn't be found. Antennas [5] and [6] did not fulfill the matching criteria. Antenna [7] was not exactly as the original, similar but just some dBs higher than original design, though antenna is good enough to work on it. Antenna [8] a parameter of the design was not specified, some trials were made but right simulations weren't reached.

On the other hand, antennas [1], [2] and [4] were simulated with very good results, even though antenna [2], have big dimensions for being an RFID tag. To this end, antennas [1], [2] and [4] were chosen for their good results in simulations, and the great bandwidth in their S_{11} and AR parameters. Their simple design is also a good point to work on them.

References

[1] Yizhu Shen, Choi L. Law, and Zhongxiang Shen, "A CPW-FED CIRUCULARLY POLARIZED ANTENNA FOR LOWER ULTRAWIDEBAND APPLICATIONS", "MICROWAVE AND OPTICAL TECHNOLOGY LETTERS", 2009, Vol. 51, No. 10, pages 2365-2369.

[2] Lin-Yu Tseng, and Tuan-Yung Han, "MICROSTRIP-FED CIRCULAR SLOT ANTENNA FOR CIRCULAR POLARIZATION", "MICROWAVE AND OPTICAL TECHNOLOGY LETTERS", 2008, Vol. 50, No. 4, pages 1056-1058.

[3] Nasimuddin, Zhi Ning Chen, and Xianming Quing, "Wideband Circularly Polarized Slot Antenna", "Radar Conference (EuRAD)", 2012, pages 504, 507.

[4] R. P. Xu, X. D. Huang, and C.H. CHeng, "BROADBAND CIRCULARYLY POLARIZED WIDE-SLOT ANTENNA", "MICROWAVE AND OPTICAL TECHNOLOGY LETTERS", 2007, Vol. 49, No. 5, pages 1005-1007.

[5] J.P. Shinde, M. D. Uplane, Raj Kumar, and P. N. Shinde, "Circularly Polarized Rectangular Slot Antenna with Trapezoidal Tuning Stub for UWB Application", "Applied Electromagnetics Conference (AEMC)", 2011, pages 1-4.

[6] Chien-Jen Wang and Chih-Hsing Chen, "CPW-Fed Stair-Shaped Slot Antennas With Circular", "IEEE TRANSACTIONS ON ANTENNAS AND PROPAGATION", 2009, Vol. 57, No. 8, pages 2486.

[7] Jia-Yi Sze, Chung-I. G. Hsu, Zhi-Wei Chen, and Chi-Chaan Chang, "Broadband CPW-Fed Circularly Polarized Square Slot Antenna With Lightening-Shaped Feedline and Inverted-L Grounded Strips", "IEEE TRANSACTIONS ON ANTENNAS AND PROPAGATION", 2010, Vol. 58, No. 3, pages 973-977.

[8] Javad Pourahmadazar, Ch. Ghobadi, J. Nourinia, Nader Felegari, and Hamed Shirzad, "Broadband CPW-Fed Circularly Polarized Square Slot Antenna With Inverted-L Strips for UWB Applications", "IEEE ANTENNAS AND WIRELESS PROPAGATION LETTERS", 2011, Vol. 10, pages 369-372.

[9] O. Ahmad Mashaal, S. K. A. Rahim, A. Y. Abdulrahman, M. I. Sabran, M. S. A. Rani, and P. S. Hall,"A Coplanar Waveguide Fed Two Arm Archimedean Spiral Slot Antenna With Improved Bandwidth","IEEE TRANSACTIONS ON ANTENNAS AND PROPAGATION", Vol. 61, No. 2, pages 939-943

3. UWB Circularly Polarized Tags Design

The chosen antennas, will be transferred to Rogers substrate (see Table 1), some design features will be tested to improve their main parameters and to set the right frequency band to test it with the radar. Also a 0.5 ns delay line will be integrated to the antennas as a proof of concept. The parameters of the substrate Rogers RO4003 are summarized in Table 3.1.

Rogers RO4003	
Permittivity ε_r	3.7
Thickness (mm)	0.813
Loss Tangent	0.002
Permeability	1
Conductor	
Thickness (µm)	35
Conductivity (S/m)	$4.1 \cdot 10^7$

Table 3.1. Rogers RO4003 data [4]

3.1. Antenna [1]

3.1.1. Antenna Design

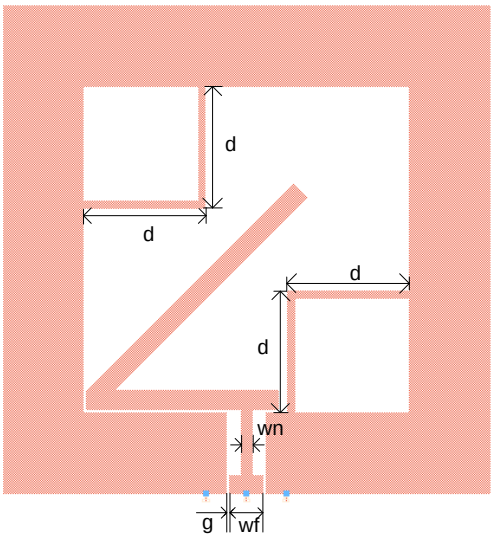

The layout of the antenna and its main dimensions are pointed out in Fig. 3.1 When substrate of the antenna was changed to Rogers, the first thing to do was changing the fed-line (*wf*, *g*) to fit an adaptation of 50 Ω, so a width of *wf*=5.7 mm and gap *g*=0.3 was selected for the simulations.

The two inverted-L grounded strips, provide the circular polarization, so they were the first parameters to be tested. Other parameters were tested but not with good or significant results except the tuning stub.

Figure 3.1. Antenna with tagged parameters which were tested.

	wf (mm)	wn (mm)	d (mm)
Antenna I	5.7	1.5	15
Antenna II	5.7	1.5	14
Antenna III	5.7	1.5	16
Antenna IV	5.7	4.5	15
Antenna V	5.7	2.9	15

Table 3.2. Modified parameters of the antenna with their respective values.

In Table 3.2, Antenna I is the original antenna but with the new fed structure. Antenna II and III are same antenna but with shorter and longer inverted-L strips (d). Antenna IV and V have the same d value but different *wn*. The results of S_{11}, axial ratio and gain are provided in Fig. 3.2, Fig.3.3 and Fig. 3.4, respectively. Antenna V was selected because its wide bandwidth of the S_{11} parameter in the frequencies which will be used, and also because it has one of the best axial ratios of all the simulations which were made, similar to Antenna I.

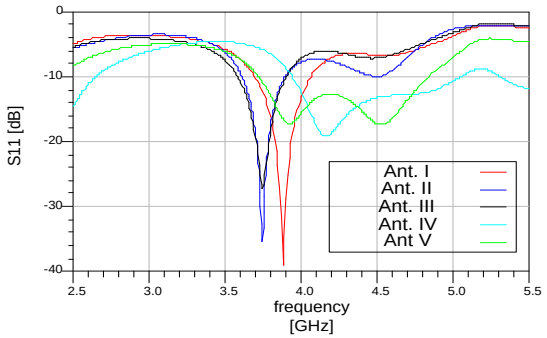

Figure 3.2. Return Loss of the designed antenna

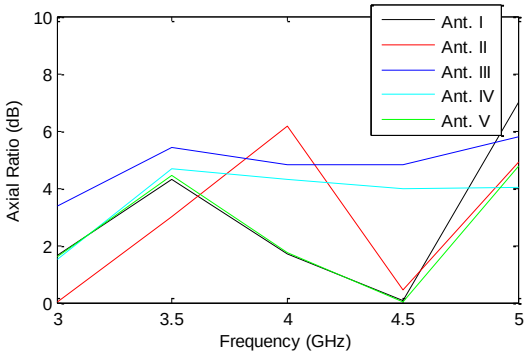

Figure 3.3. Axial Ratio of the designed antenna.

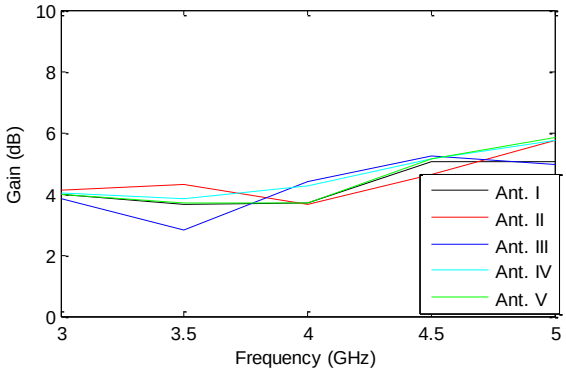

Figure 3.4. Gain of the designed antenna

3.1.2. Delay Line Design

The function of the delay line is to separate the tag mode from structural mode in time domain. In order to do that the selected delay will be 1ns, but that means to design a delay line of 0.5 ns because it will be traversed twice. First we have:

$$t = \frac{l}{v}\ [s] \tag{3.1}$$

Where *t* is the delay time (s), *l* is the length of the line (m), and *v* is the speed of propagation of the electromagnetic wave. The parameter we are looking for is ***l*,** in order to do that the other two parameters must be known**,** *t* will be 0.5 ns as it was mentioned before, and *v* can be found using the next formula:

$$v = \frac{c}{\sqrt{\varepsilon_{eff}}}\ [m/s] \tag{3.2}$$

Where c is the speed of light in the vacuum (3e8 m/s), and ε_{eff} is the effective dielectric constant. The latter is not known, but it can be calculated using LineCalc tool of ADS entering all the values of the substrate and selecting a Microstrip structure. The value obtained for ε_{eff} is 2.872. Now all values are known, (3.1) and (3.2) can be put together, and *l* isolated:

$$l = \frac{t \cdot c}{\sqrt{\varepsilon_{eff}}} = \frac{0.5 \cdot 10^{-9}[s] \cdot 3 * 10^{8}[m/s]}{\sqrt{2.872}} = 0.08851\ [m] \tag{3.3}$$

On the other hand, ADS does not allow for an automatic design of a delay line for a CPW structure, so LineCalc tool was used to find an impedance which matched the fed-line of the antenna, but selecting a Microstrip structure as it's shown in Figure 3.5. The impedance selected was 21.47 Ω

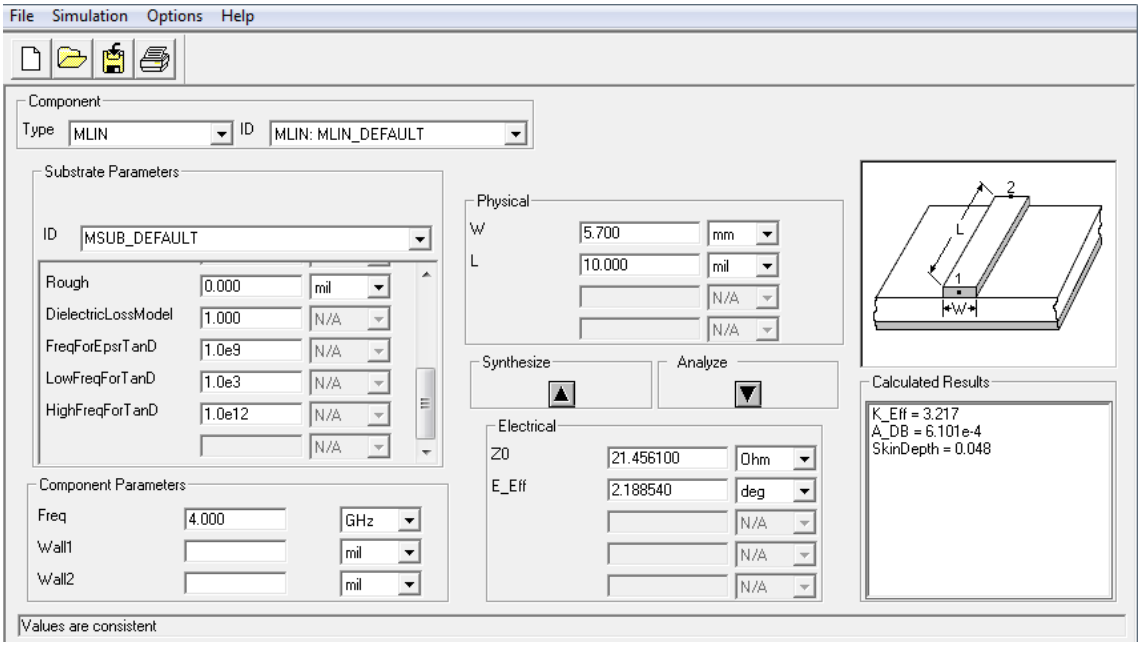

Figure 3.5. Generating the value ε_{eff} with LineCalc tool.

After that, the Design Guide for passive circuits of ADS was used to generate the delay line. The values of the impedance mentioned before, the substrate characteristics (Table 3.1), the physical length calculated before, a central frequency of 4 GHz and dimensions of 40x40 mm were used for the design of the delay line, which is the one shown in Figure 3.6.

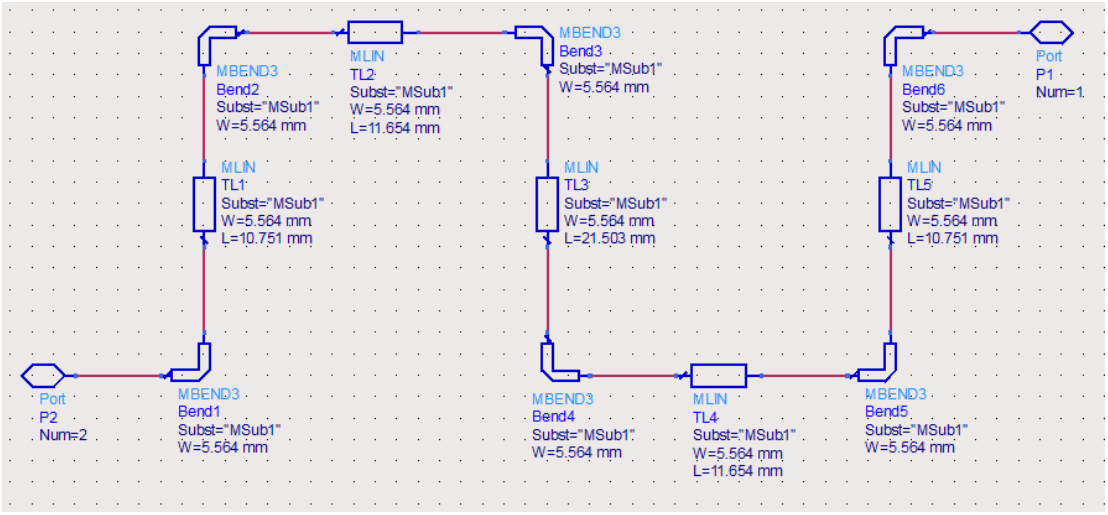

Figure 3.6. Dimensions of the delay line.

Simulations of the S_{11} and S_{21} parameters and the delay are given in Fig. 3.7, Fig. 3.8 and Fig. 3.9, respectively.

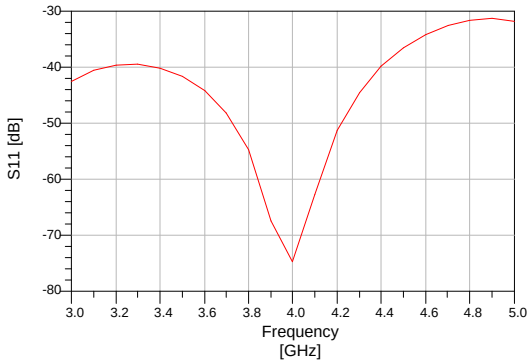

3.7. Return Loss of the delay line.

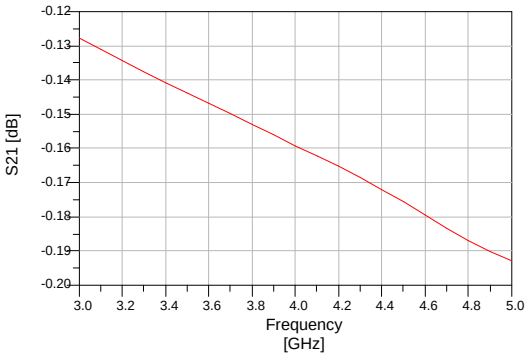

3.8. S_{21} parameter of the delay line

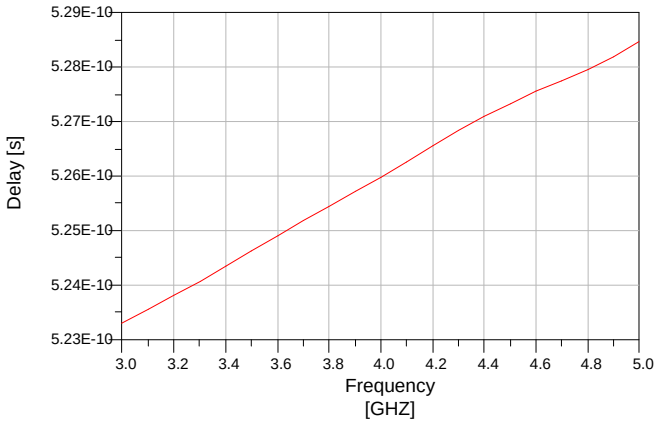

3.9. Delay time of the delay line.

3.1.3. Integration of the Delay Line to the Antenna

Once the antenna was selected, and the delay line designed, the layout of the delay line was generated and modified to match the fed-line of the antenna and to become a CPW structure just like the antenna itself. After all these modifications both structures were connected and the result is the one shown in Figure 3.10.

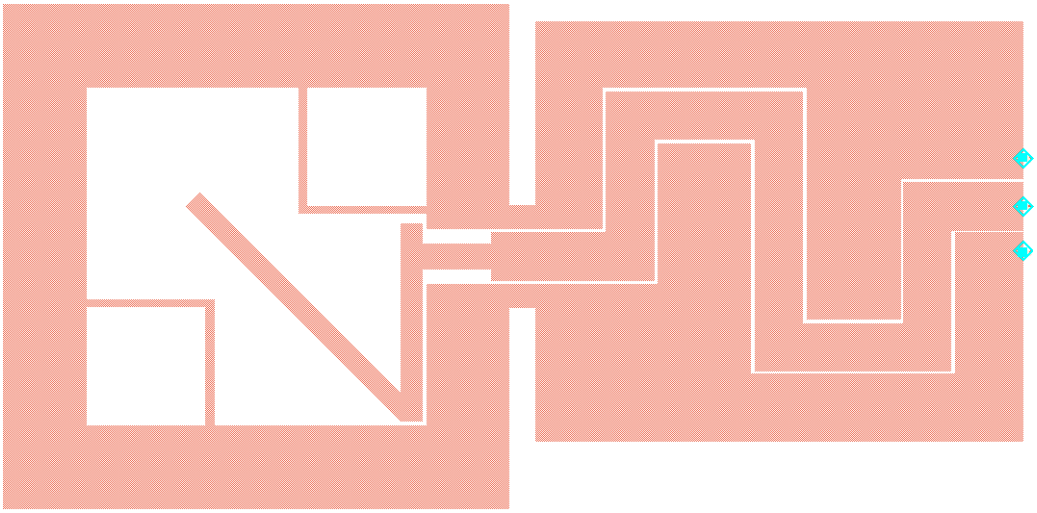

Figure 3.10. Antenna with a delay line integrated.

The simulated S_{11} parameter of the tag is shown in Fig. 3.11. Good matching can still be found between 3.3 and 4.5 GHz. The axial ratio is provided in Fig. 3.12 and the simulated gain in Fig. 3.13. Integrating delay lines in UWB antennas is very critical and the parameters of the antenna always worsen. In consequence, the results for this tag can be considered satisfactory and is a good candidate to be manufactured.

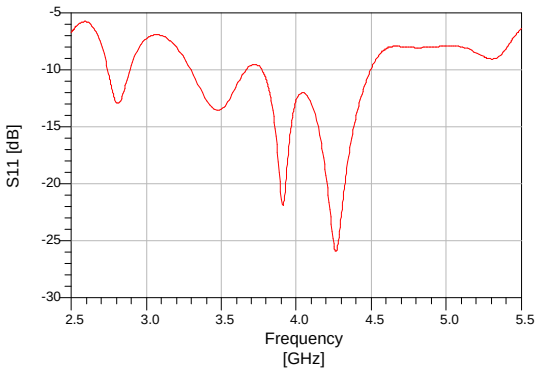

Figure 3.11. Return loss of the antenna with a delay line integrated.

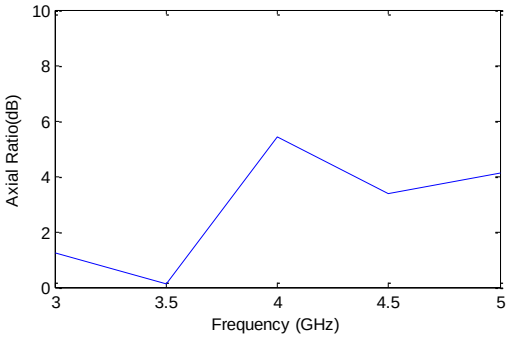

Figure 3.12. Axial Ratio of the antenna with a delay line integrated

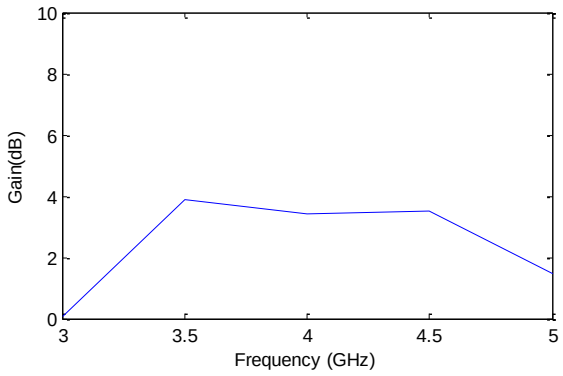

Figure 3.13. Gain of the antenna with a delay line integrated

3.2 Antenna [2]

3.2.1 Antenna Design

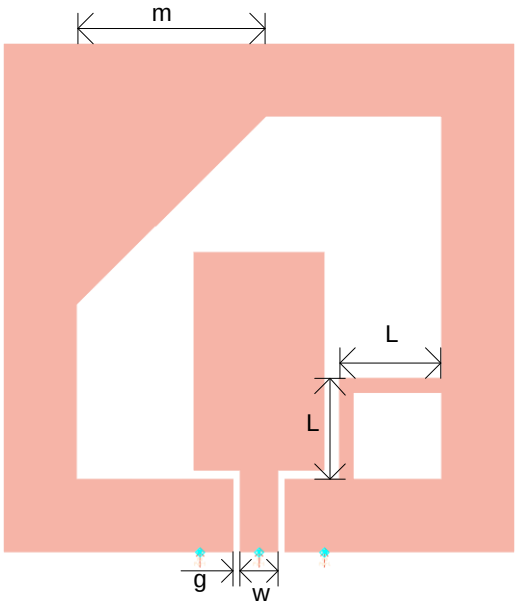

Figure 3.14. Antenna with tagged parameters which were tested.

The layout of the antenna and its main dimensions are pointed out in Fig. 3.14. This antenna was fed originally with 60 Ω so the fed-line is a bit thinner than in the previous case. As in the former case the Axial Ratios of the antenna was achieved by the inverted-L strip and the truncated corner, so these were the parameters which were first tested. On the other hand there was not much space inside the antenna especially for the L-inverted strip so not many trials could be done. Other parameters have been tested but not with significant results, so they are not included here. The three prototypes more significant for this study are provided in Table 3.3, where the parameters that have been changed are pointed out.

	w (mm)	L (mm)	m (mm)
Antenna I	5.6	7	13
Antenna II	5.6	6.5	12.5
Antenna III	5.6	7.5	13.5

Table 3.3. Modified parameters of the antenna with their respective values.

As can be observed in the simulations of Fig. 3.15-16 return loss has almost the same bandwidth under 10 dB in the three cases but axial ratio has a better behavior in Antenna II, so this antenna is selected.

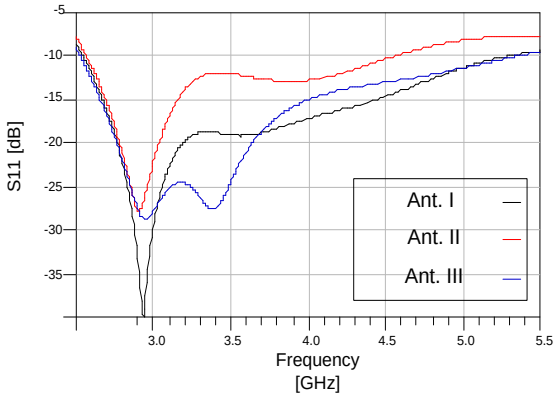

Figure 3.15. Return Loss of the designed antenna

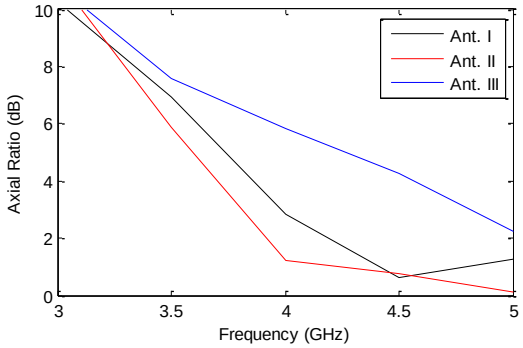

Figure 3.16. Axial Ratio of the designed antenna

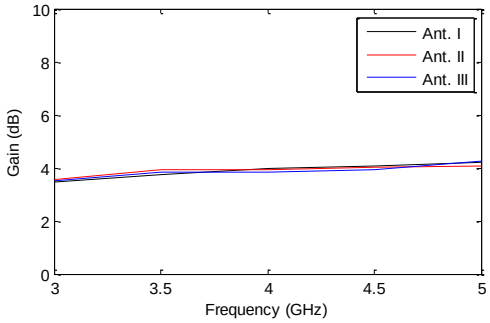

Figure 3.17. Gain of the designed antenna

3.2.2. Delay Line Design

Once the antenna is selected, the delay line must be designed, parameters are almost equal to the previous case, but at this time with an impedance of 37.65 Ω. The structure of the delay line is the one in Figure 3.18.

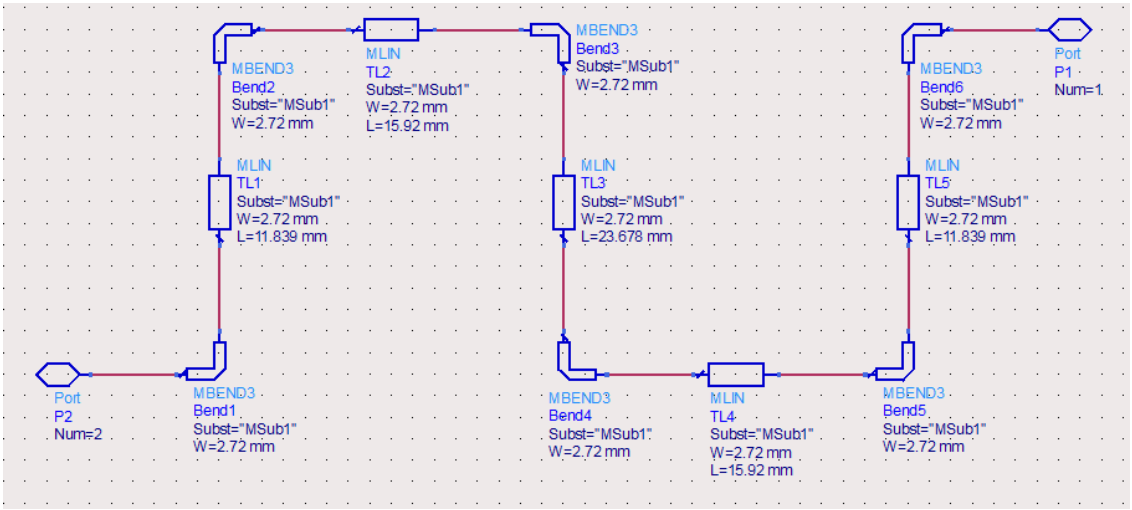

Figure 3.18. Dimensions of the delay line.

Simulations of the parameters S_{11} and S21and the delay are provided in Fig. 3.19, Fig. 3.20 and Fig. 3.21, respectively.

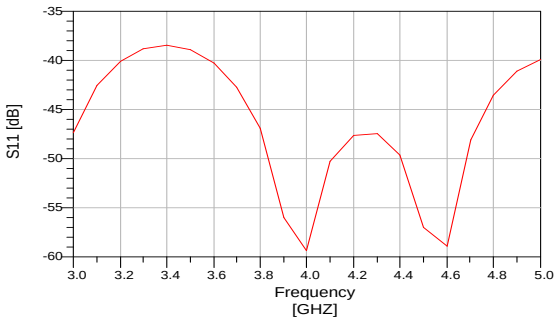

Figure 3.19. Return Loss of the delay line.

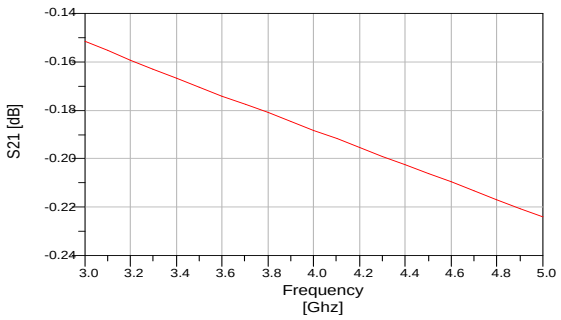

Figure 3.20. S21 Parameter of the delay line.

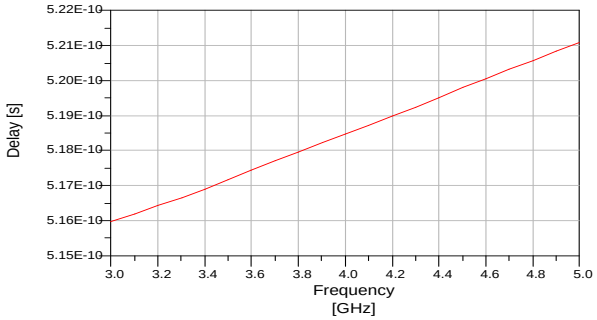

Figure 3.21. Delay time of the delay line.

3.2.3. Integration of the delay Line to the Antenna

Just like in last case the delay line structure had to be modified to match the antenna structure. The final tag the design is the one in Figure 3.2.9.

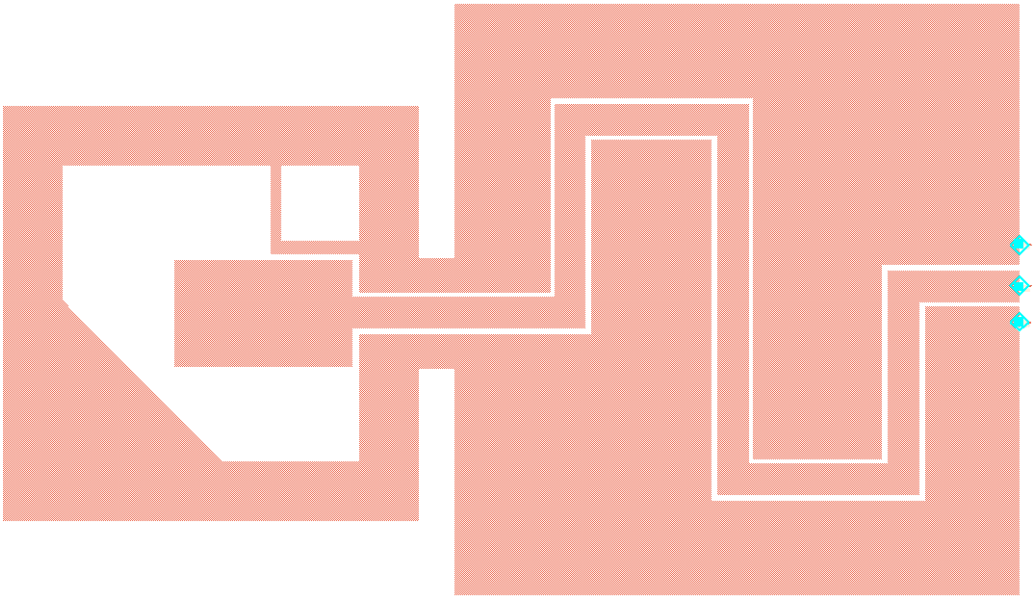

Figure 3.22. Antenna with a delay line integrated.

In figures below simulations of the main parameters of the final antenna can be shown, the parameters have also changed because the integration of the delay line. Return loss (figure 3.23) is still good and offers a good bandwidth (more than 2 GHz) but Axial Ratio (Fig. 3.24) has become worse, nevertheless still seems a good antenna to manufacture. The simulated gain is shown in Fig. 3.25.

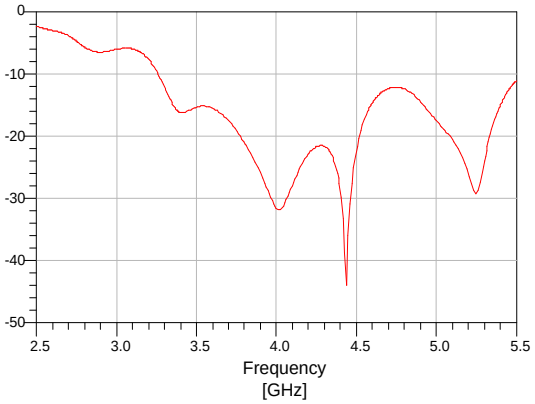

Figure 3.23. Return loss of the antenna with a delay line integrated.

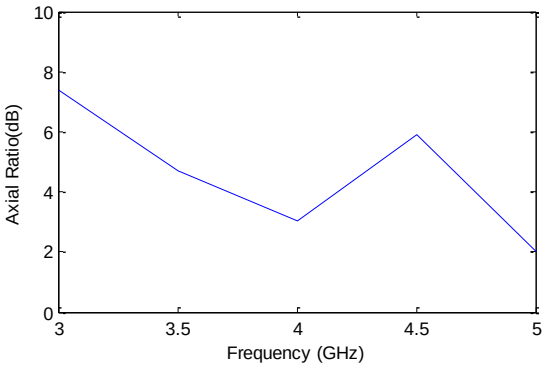

Figure 3.24. Axial ratio of the antenna with a delay line integrated.

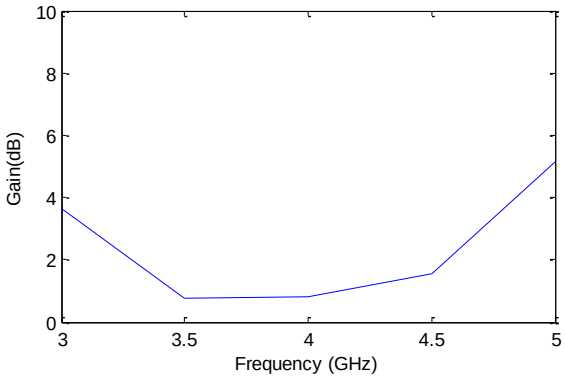

Figure 3.25. Gain of the antenna with a delay line integrated.

3.3. Antenna [3]

3.3.1 Antenna Design

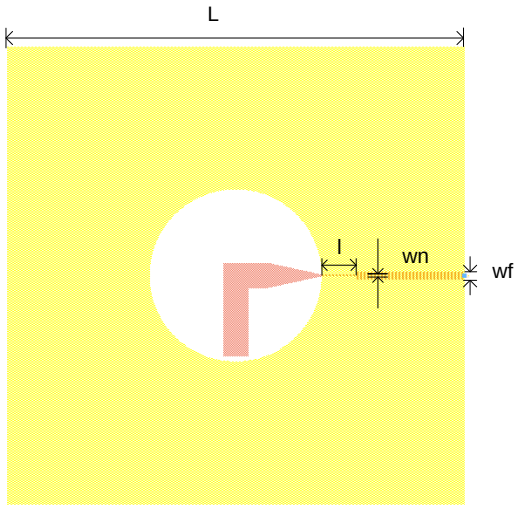

Figure 3.26. Antenna with tagged parameters which were tested.

The layout of the antenna and its main dimensions are pointed out in Fig. 3.26. The width of the microstrip fed-line was set to 1.73 mm (50 Ω). This antenna is completely different to the previous designs so many parameters were tested but just the three parameters of Table 3.4 showed significant differences in their simulations. First parameter *l* was tested but return loss became worse, after that parameter *wn* showed a lot of different results, the smaller it was, the better results in return loss parameter, so it was set to 0.4 mm because it could be difficult to manufacture it. After that parameter, varying *L* and making it longer, return loss bandwidth increased at lower frequencies, so after several simulations it was set to 124 mm, but that could make a maybe too big antenna for a RFID design, so both Antenna III and Antenna IV were selected.

	wf (mm)	l (mm)	wn (mm)	L (mm)
Antenna I	1.73	7.2	0.5	100
Antenna II	1.73	5.2	0.5	100
Antenna III	1.73	7.2	0.4	100
Antenna IV	1.73	7.2	0.4	124

Table 3.4. Modified parameters of the antenna with their respective values.

As can be observed in the simulations of Fig. 3.27, return loss bandwidth under 10 dB is enhanced around 300 MHz in Antenna VII respect Antenna I and III. In Fig. 3.28 can be seen that axial ratio has excellent results in each case through all the bandwidth. Finally in Fig. 3.29 gain of all the antennas can be seen.

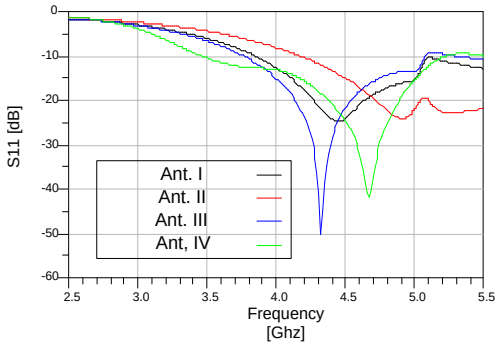

Figure 3.27. Return Loss of the designed antenna.

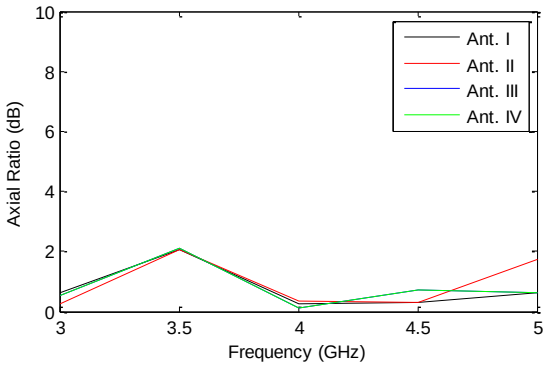

Figure 3.28. Axial ratio of the designed antenna.

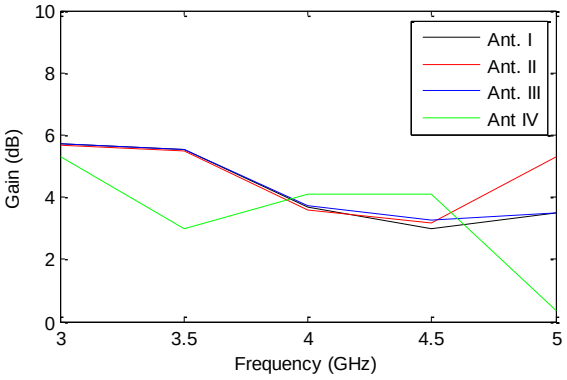

Figure 3.29. Gain of the designed antenna.

3.3.2. Delay Line Design

This antenna is designed in a *Microstrip* structure so it was easier to design with ADS, same parameters as in former tags were entered but this time with the real impedance of the antenna 50 Ω, there was not a need to use *Linecalc* for this case. The structure of the delay line is the one in Figure 3.30.

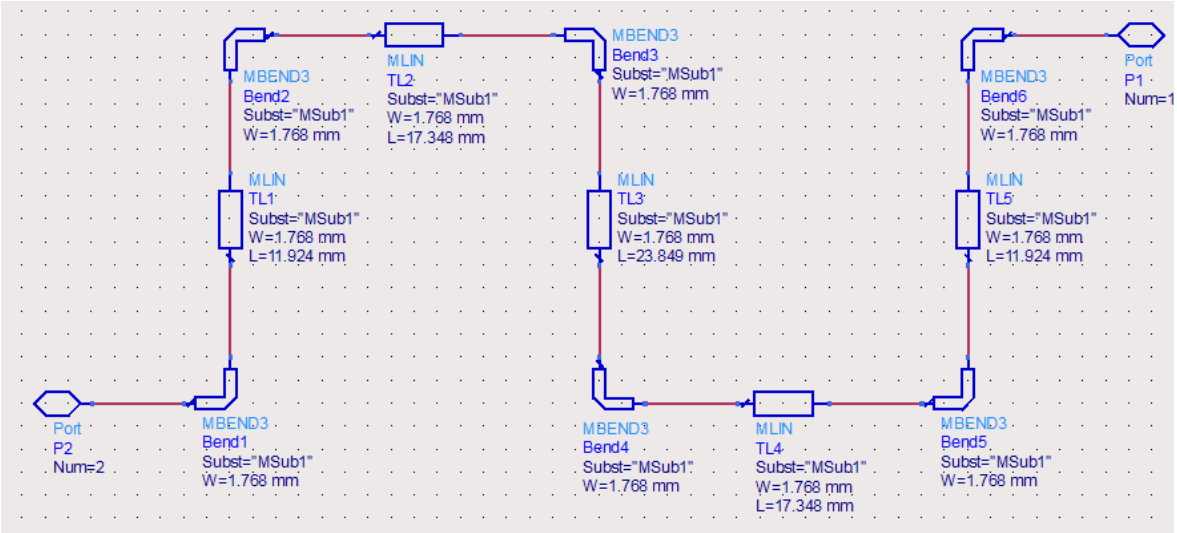

Figure 3.30. Dimensions of the delay line.

Simulations of the parameters S_{11} and S21and the delay are provided in Fig. 3.31, Fig. 3.32 and Fig. 3.33, respectively.

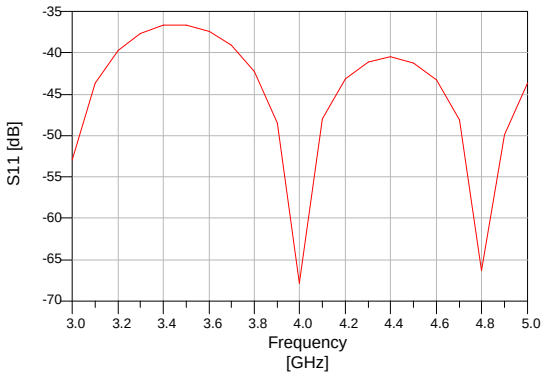

Figure 3.31. Return Loss of the delay line

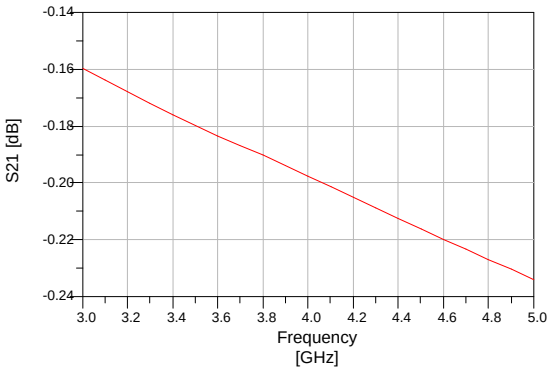

Figure 3.32. S21 Parameter of the delay line

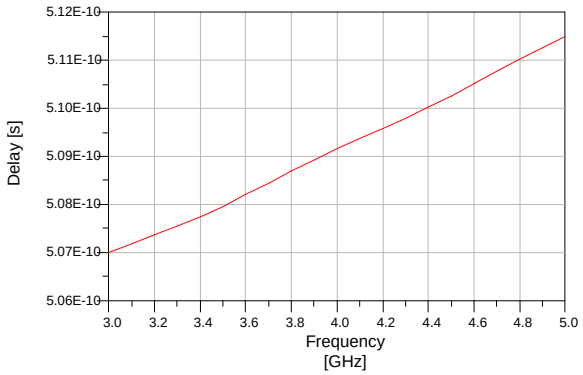

Figure 3.33. Delay time of the delay line

3.3.3. Integration of the Delay Line to the Antenna

This case was easier than other cases, the antenna was fed with microstrip line, so not many modifications had to be made to integrate the two structures and obtain the tags. The final designs can be seen in Figure 3.3.9.

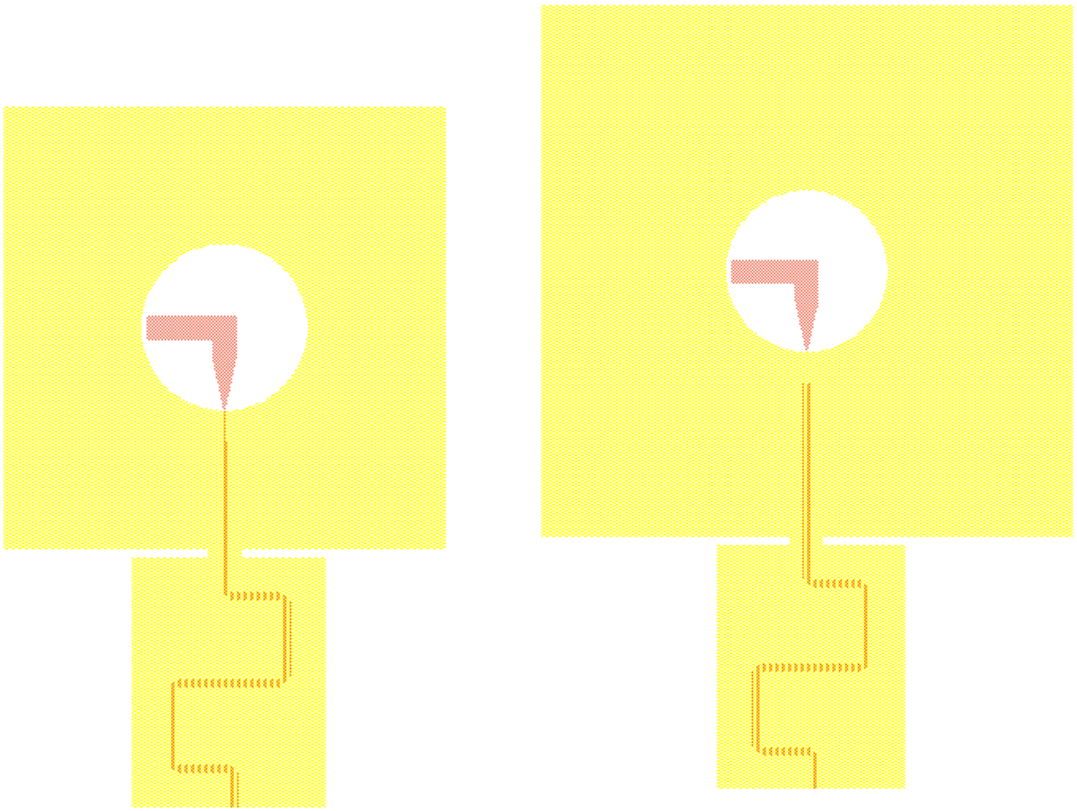

(a) 100x100 mm antenna **(b)** 124x124 mm antenna

Figure 3.34. Antenna with a delay line integrated.

In figures below simulations of the main parameters of the two final tags (Antenna III and Antenna IV with delay lines) can be shown, the parameters have changed again because the integration of the delay line. Return loss (figure 3.35) and axial ratio parameters (Figure 3.36) are similar to the antennas without the delay lines and offer a wide bandwidth, so the delay lines were integrated with succeed. The gain is given in Fig. 3.37.

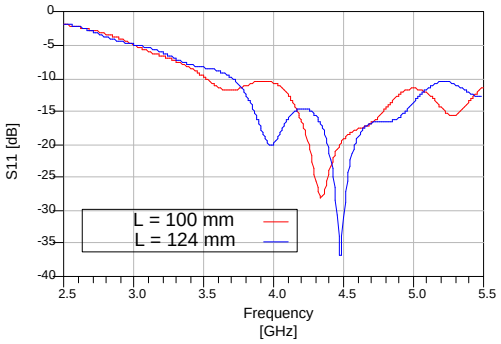

Figure 3.35. Return loss of both antennas with a delay line integrated.

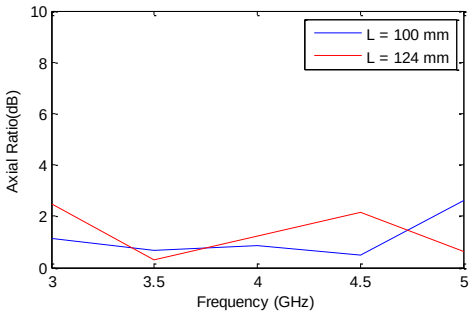

Figure 3.36. Axial Ratio of both antennas with a delay line integrated.

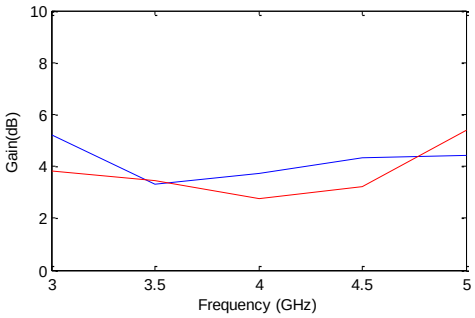

Figure 3.37. Gain of both antennas with a delay line integrated.

References

[1] Jia-Yi Sze, Chung-I. G. Hsu, Zhi-Wei Chen, and Chi-Chaan Chang, "Broadband CPW-Fed Circularly Polarized Square Slot Antenna With Lightening-Shaped Feedline and Inverted-L Grounded Strips", "IEEE TRANSACTIONS ON ANTENNAS AND PROPAGATION", 2010, Vol. 58, No. 3, pages 973-977.

[2] Yizhu Shen, Choi L. Law, and Zhongxiang Shen, "A CPW-FED CIRUCULARLY POLARIZED ANTENNA FOR LOWER ULTRAWIDEBAND APPLICATIONS", "MICROWAVE AND OPTICAL TECHNOLOGY LETTERS", 2009, Vol. 51, No. 10, pages 2365-2369.

[3] Lin-Yu Tseng, and Tuan-Yung Han, "MICROSTRIP-FED CIRCULAR SLOT ANTENNA FOR CIRCULAR POLARIZATION", "MICROWAVE AND OPTICAL TECHNOLOGY LETTERS", 2008, Vol. 50, No. 4, pages 1056-1058.

[4] Rogers Corporation, RO4000 Series Datasheet, http://www.rogerscorp.com/documents/726/acm/RO4000-Laminates---Data-sheet.pdf

4. Measures of Chipless RFID Tags

4.1. Measurement System

The system which was built for these measures [1] is the one shown in Fig. 4.1. As it was said in Chapter 2, a radar will be used as reader. This radar will include two antennas, one for transmission and another for reception; these two antennas are linearly polarized, and both with the same polarization. This radar will be connected to the computer, which will process the data with a Matlab routine. The tag to be tested will be placed in the top of a rotor and both of them inside a semi-anechoic chamber, which is not closed in three of their sides, but it helps to diminish multipath effects.

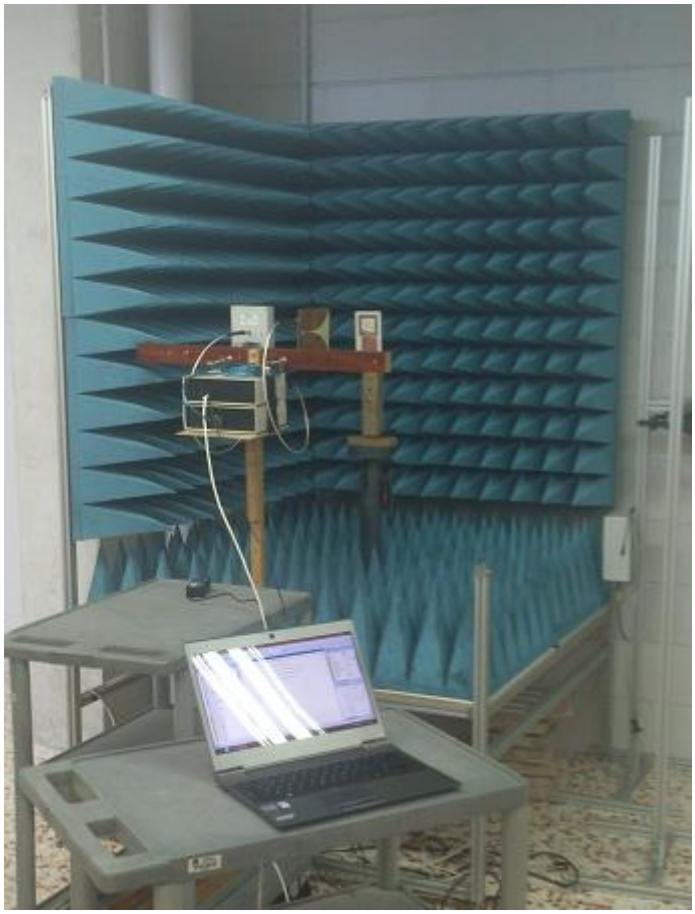

Figure 4.1. Picture of the measure system

For distance measures the radar will be placed in a cart, in order that when we move the cart the distance between the radar and the tag increases, and so that we can know how far we can go to read the tag correctly.

In last measures the radar will be placed just above the tag, and with another Matlab routine, the rotary motor will be controlled achieving with that, measures of all the angles (steps of 2º), and testing if the antenna is actually well polarized. The schema of the measurement set-up is shown in Fig. 4.2.

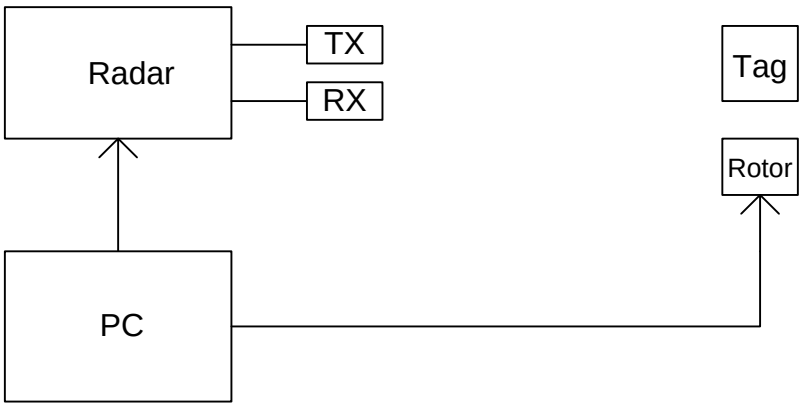

Figure 4.2. Schema of the measuring system

4.2. Tag 1

Tag 1 is the one that has been designed and explained in Section 3.1. The photograph of the manufactured prototype is shown in Fig. 4.3.

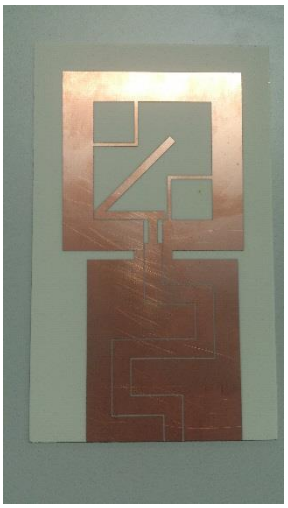

Fig. 4.3. Photograph of the manufactured prototype Tag 1.

First thing to do was measuring the structural and tag mode for the selected tag in both polarizations. In both cases (Figure 4.4 and Figure 4.5), the two modes were easy detected and the delay time between them was 1.7 ns. This delay is larger than the one designed since it also accounts for the delay of the antenna.

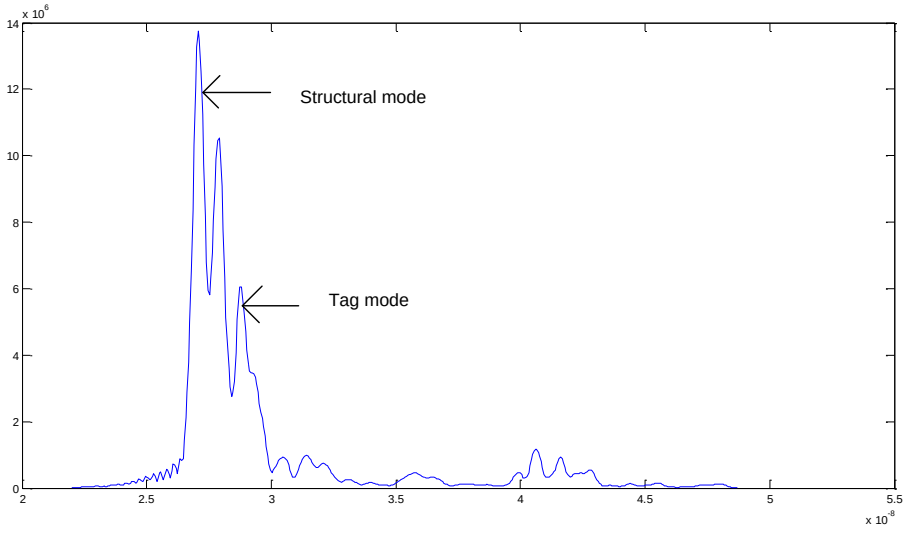

Figure 4.4. Structural and tag mode received from the tag in a vertical position.

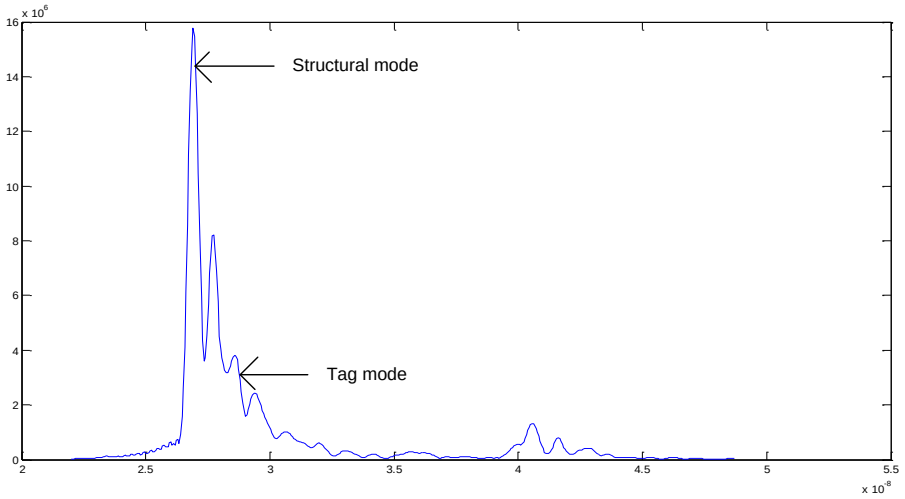

Figure 4.5. Structural and tag mode received from the tag in a horizontal position.

These measures have been processed with a Matlab routine which first asks, for the background (without the antenna), and then asks for the tag measurement. In this way the processing steps are: 1/ background subtraction (the empty-room measurement is subtracted from the measurement with the tag) and 2/ the wavelet transform is applied in order to minimize noise [1].

In next figures (Fig. 4.6 to 4.8) there are plots, of the tag in a vertical position and in distances between 40 cm and 190 cm; the tag mode can be easily seen in all distances.

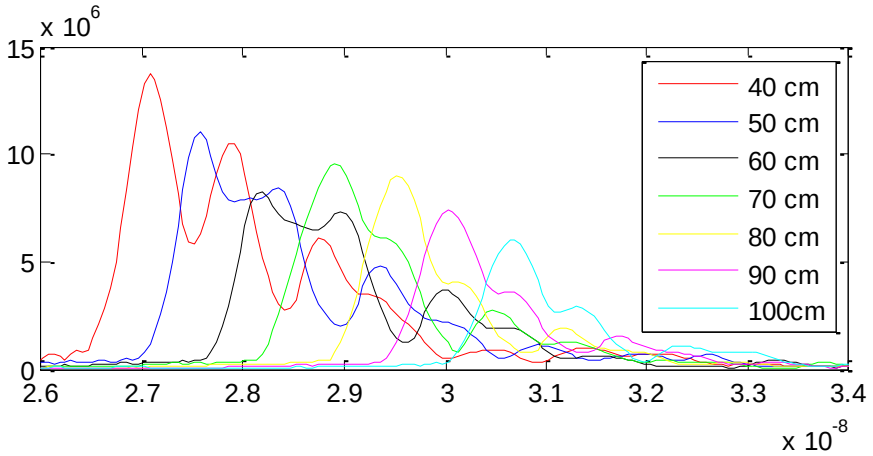

Figure 4.6. Signal received by the UWB radar in distances between 40 and 100 cm

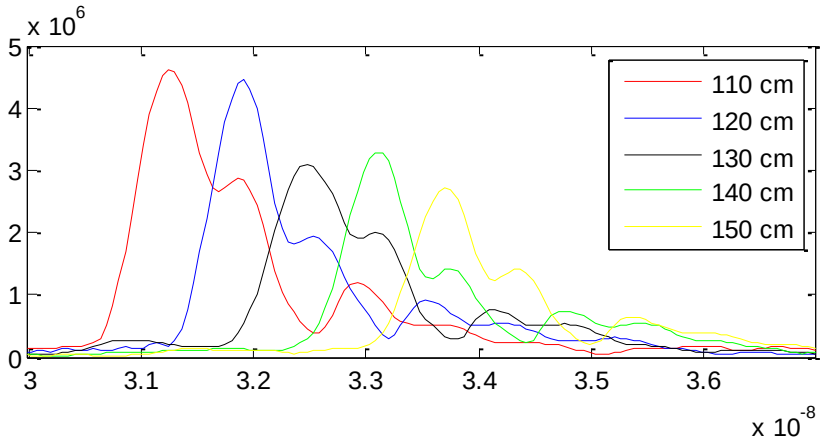

Figure 4.7. Signal received by the UWB radar in distances between 110 and 150 cm

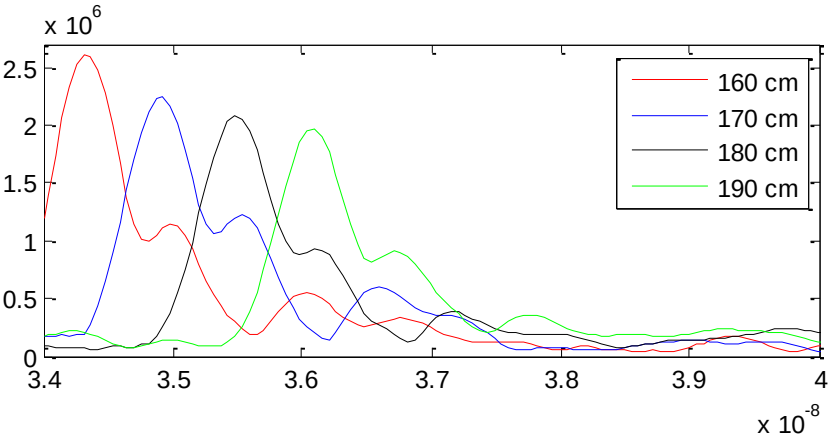

Figure 4.8. Signal received by the UWB radar in distances between 160 and 190 cm

In next figures (Fig. 4.9 to Fig. 4.11) there are plots of the tag in a horizontal position and in distances between 40 cm and 200 cm; tag mode can also be seen in all distances.

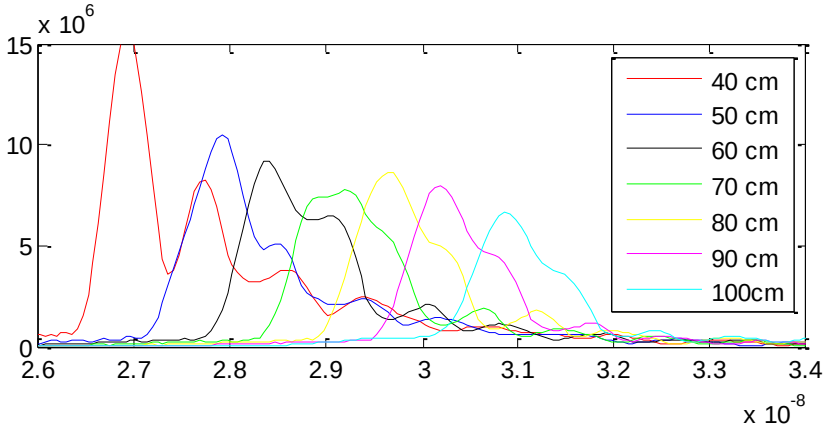

Figure 4.9. Signal received by the UWB radar in distances between 40 and 100 cm

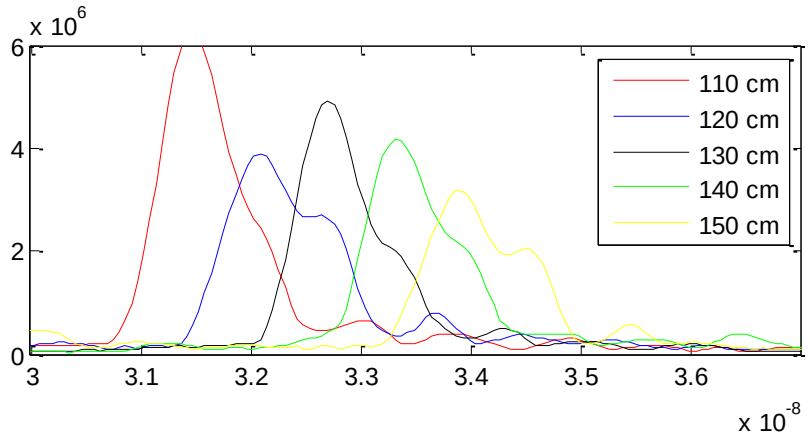

Figure 4.10. Signal received by the UWB radar in distances between 110 and 150 cm

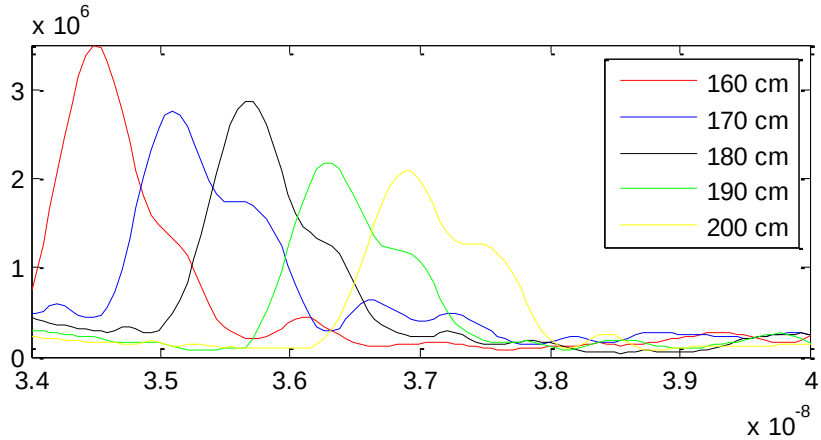

Figure 4.11. Signal received by the UWB radar in distances between 160 and 200 cm

In next figures (Fig. 4.12 to Fig. 4.14) there are plots, of the tag declined 45º from de horizontal position and in distances between 40 cm and 200 cm; tag mode can also be seen in all distances.

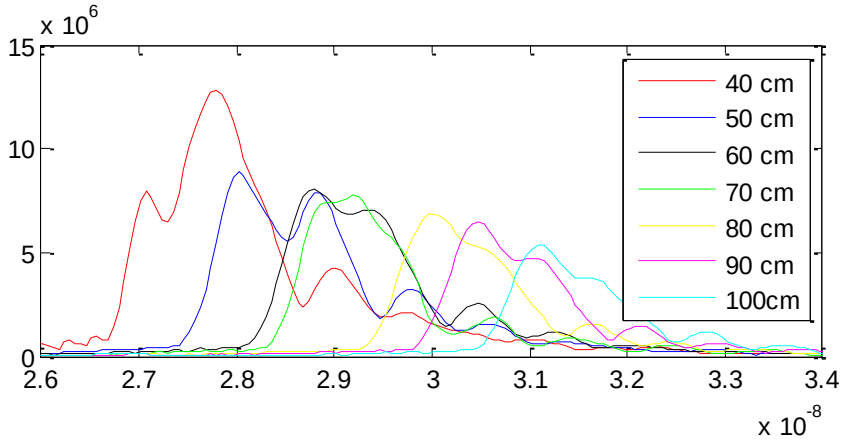

Figure 4.12. Signal received by the UWB radar in distances between 40 and 100 cm

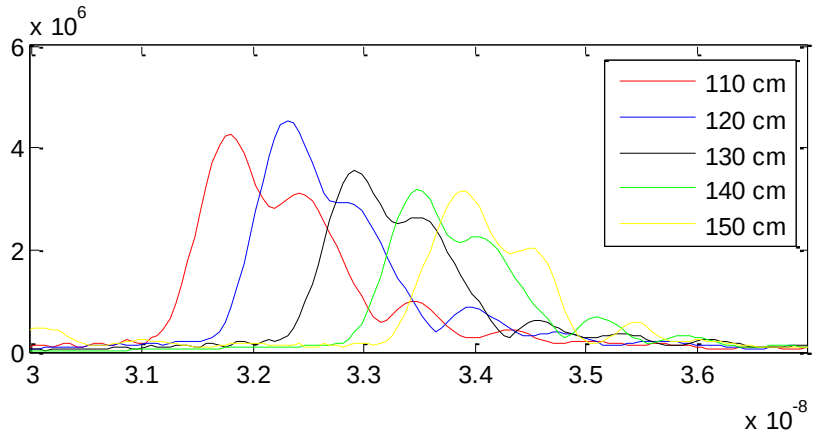

Figure 4.13. Signal received by the UWB radar in distances between 110 and 150 cm

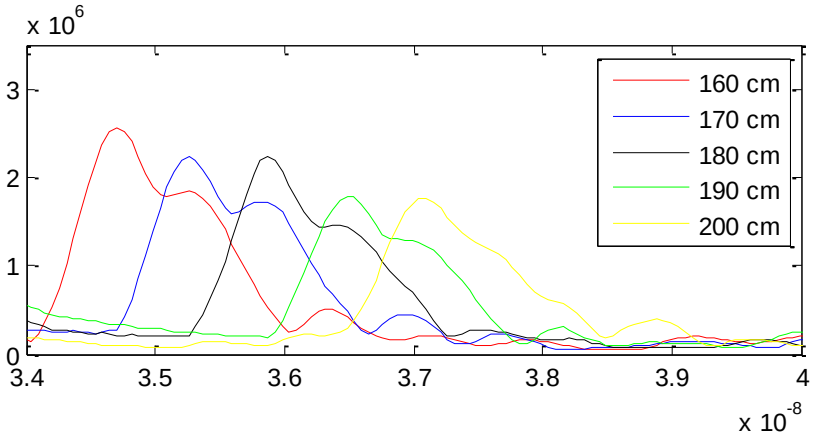

Figure 4.14. Signal received by the UWB radar in distances between 160 and 200 cm

Finally the tag was tested for all angles using the rotary motor as explained above. The result was compared to a balloon-shaped antenna (Figure 4.16) and to Vivaldi (Figure 4.17) antennas. Vivaldi antenna is the extreme case, since it is a very linearly-polarized antenna. It can be easily seen that at +/- 90 degrees the tag mode cannot be detected while at 0 degrees it can be read. On the other hand the balloon antenna is also linearly polarized, and its minimum values are more than 5 dB below its maximum values. The RFID tag that has been designed has almost no loss between its maximum and its minimum values (around 2 dB) which it means the tag has actually a good circular polarization.

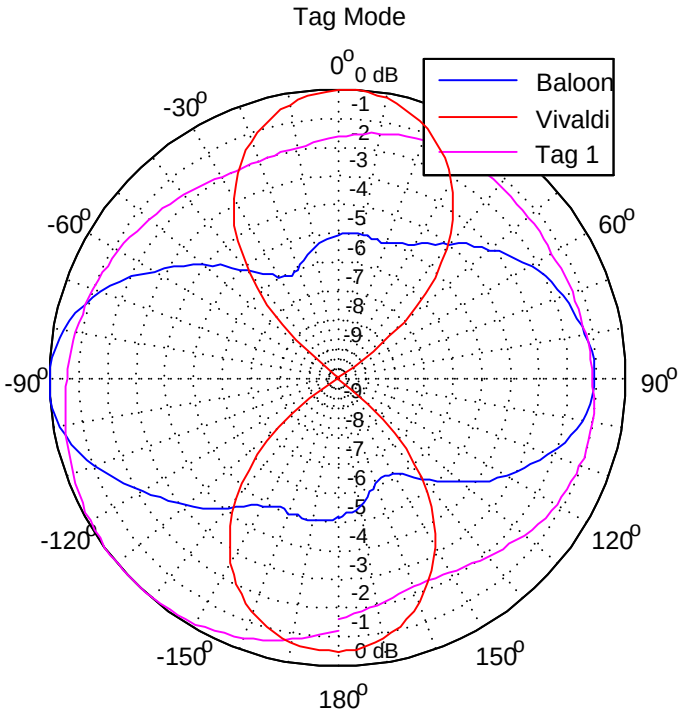

Figure 4.15. Normalized radiated power of the three antennas in all angles.

Figure 4.16. Balloon antenna.

Figure 4.17. Vivaldi antenna.

4.3. Tag 2

Tag 2 is the one that has been designed and explained in Section 3.2. The photograph of the manufactured prototype is shown in Fig. 18.

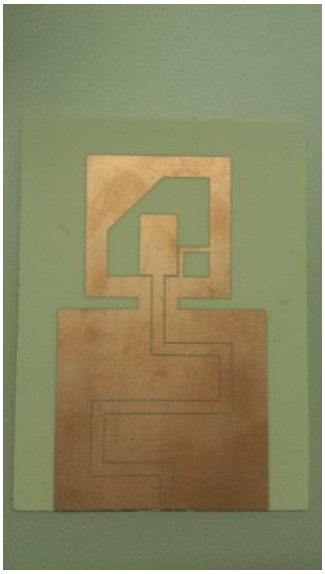

Figure 4.18. Tag 2

First thing to do was measuring the structural and tag mode for the selected tag in both polarizations. In both cases (Figure 4.19. and Figure 4.20.), the two modes were easy to see and the delay time between them was 1.9 ns.

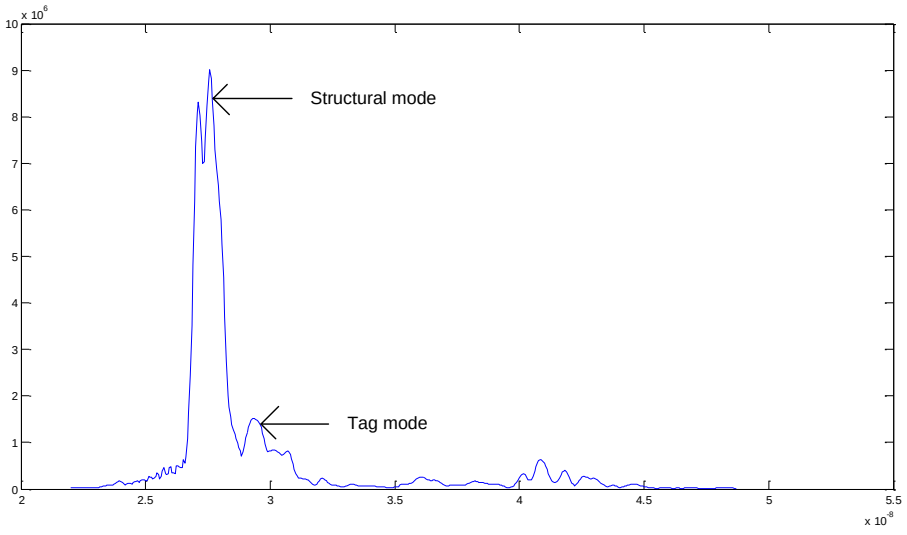

Figure 4.19. Structural and tag mode received from the tag in a vertical position.

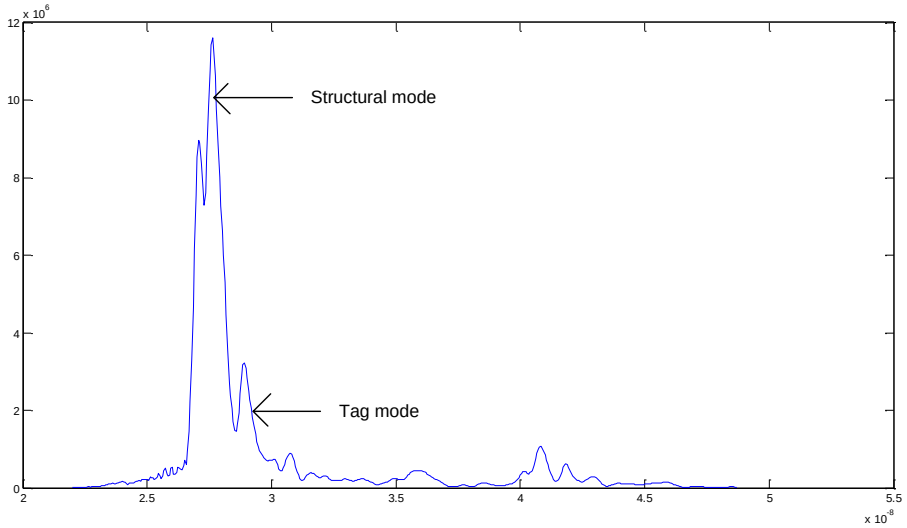

Figure 4.20. Structural and tag mode received from the tag in a horizontal position.

In next figures (Fig. 4.21 to Fig. 4.23) there are plots, of the tag in a vertical position and in distances between 40 cm and 200 cm, this time tag mode is hard to see for more than 150 cm:

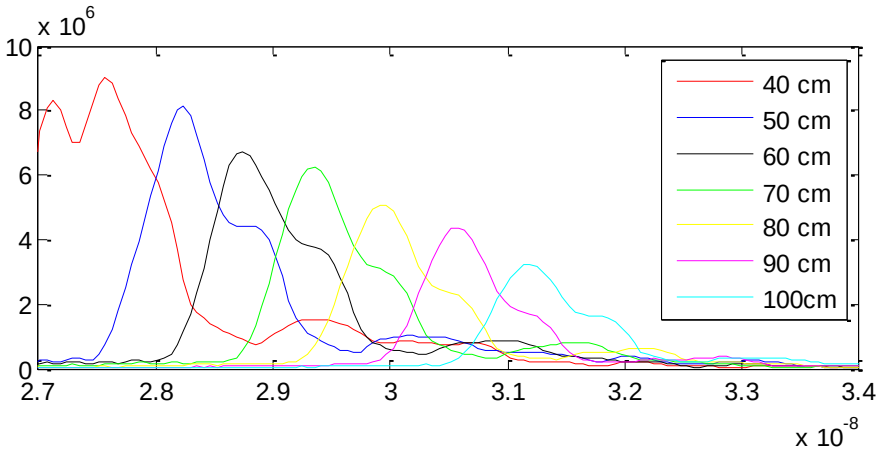

Figure 4.21. Signal received by the UWB radar in distances between 40 and 100 cm.

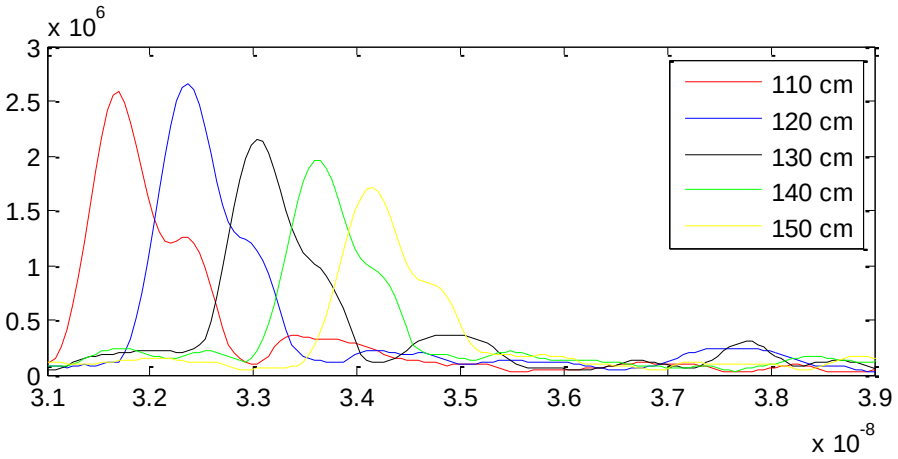

Figure 4.22. Signal received by the UWB radar in distances between 110 and 150 cm.

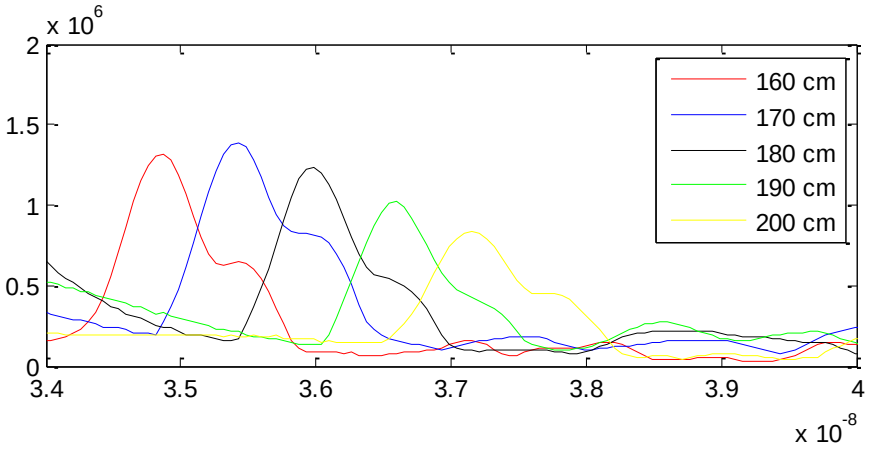

Figure 4.23. Signal received by the UWB radar in distances between 160 and 200 cm.

In next figures (Fig. 4.24 to Fig. 4.26) there are plots, of the tag in a horizontal position and in distances between 40 cm and 2 meters, this time, tag mode is higher than last case, but again if the distance is more than 150 cm, it is hard to see :

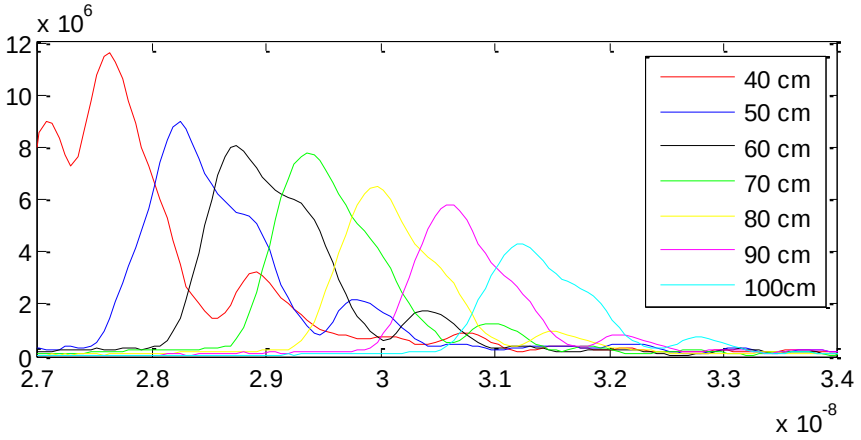

Figure 4.24. Signal received by the UWB radar in distances between 40 and 100 cm

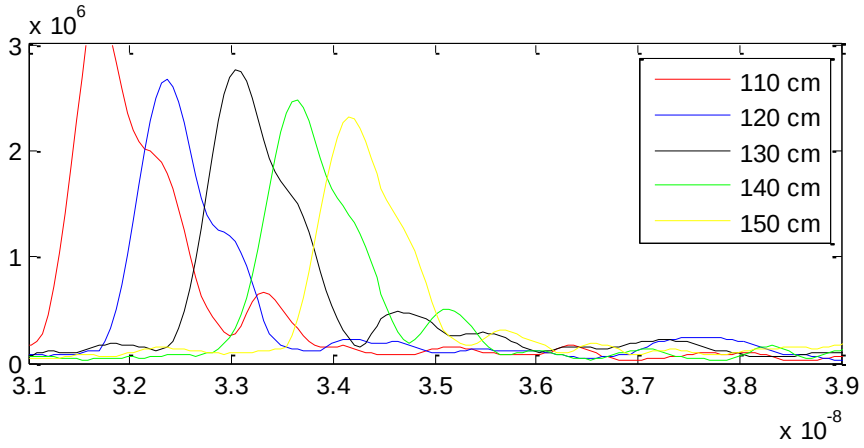

Figure 4.25. Signal received by the UWB radar in distances between 110 and 150 cm.

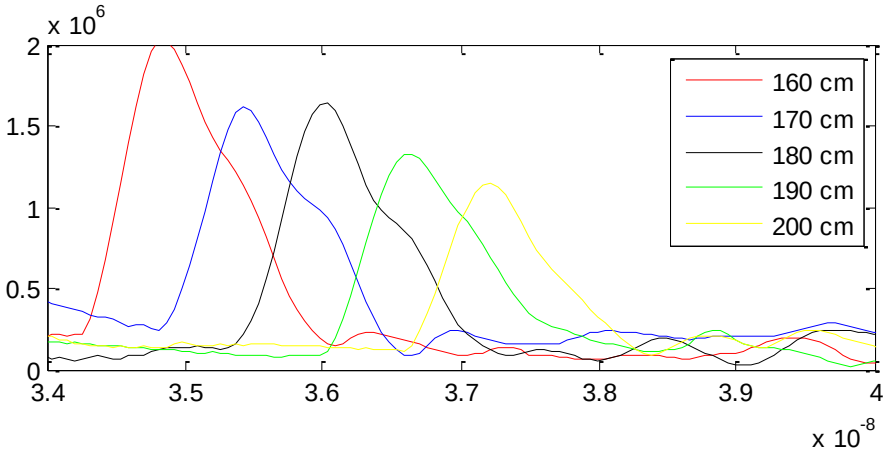

Figure 4.26. Signal received by the UWB radar in distances between 160 and 200 cm.

Finally the Tag 2 was tested for all angles just like with the other tag, and comparing it again with the other two antennas. This RFID tag it's not as good as the last one but it has also a good polarization, having differences between its maximum and minimum around 2 dB.

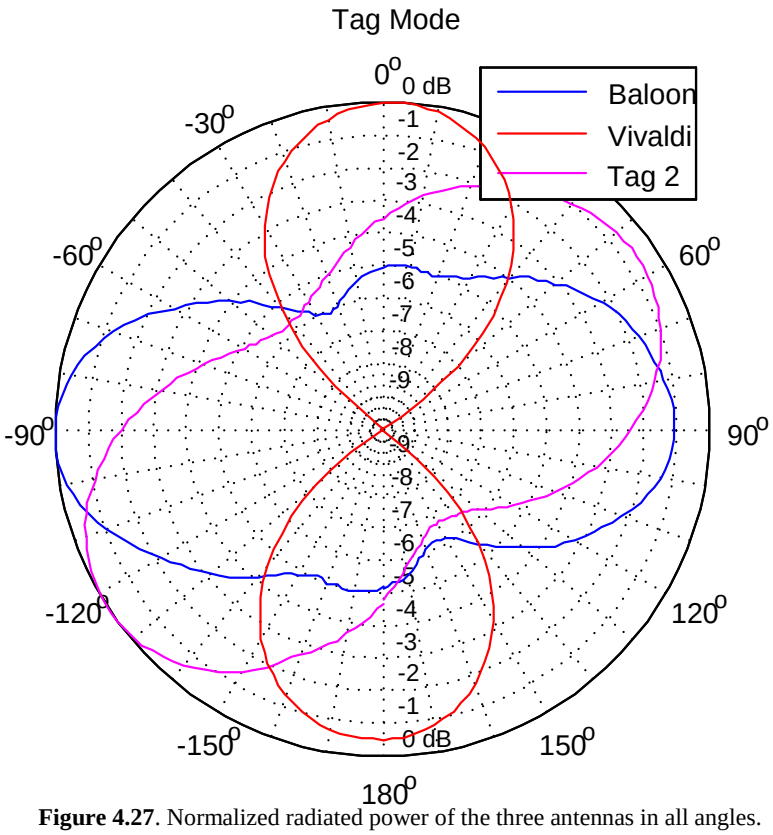

Figure 4.27. Normalized radiated power of the three antennas in all angles.

4.4. Tag 3

Tag 2 is the one that has been designed and explained in Section 3.3. The photograph of the manufactured prototype is shown in Fig. 4.3.

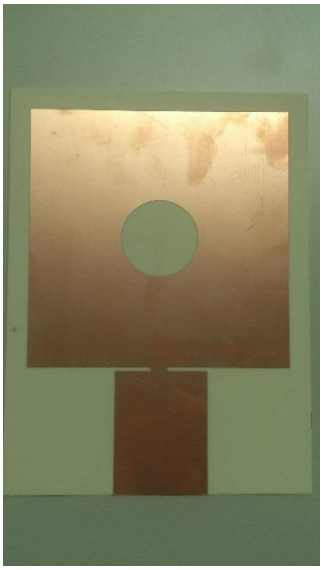

Figure 4.28. Top of Tag 3

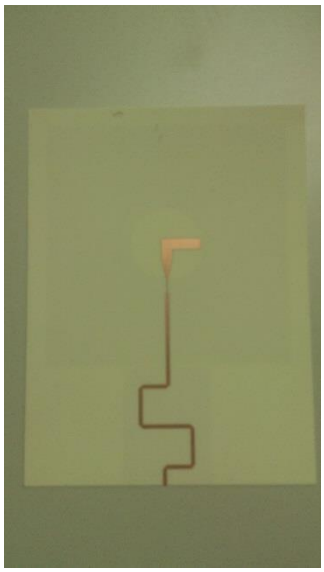

Figure 4.29. Bottom of Tag 3

Due to the large size of this tag, its structural mode is too big so it made the tag mode undistinguishable from the structural mode; after a few trials, the size of the tag was reduced

but it remained undistinguishable. Finally it was decided to cut the delay line, and measure only the antenna connected to a coaxial delay line in order to evaluate the antenna performance. The angular measurement is shown in Fig.30.

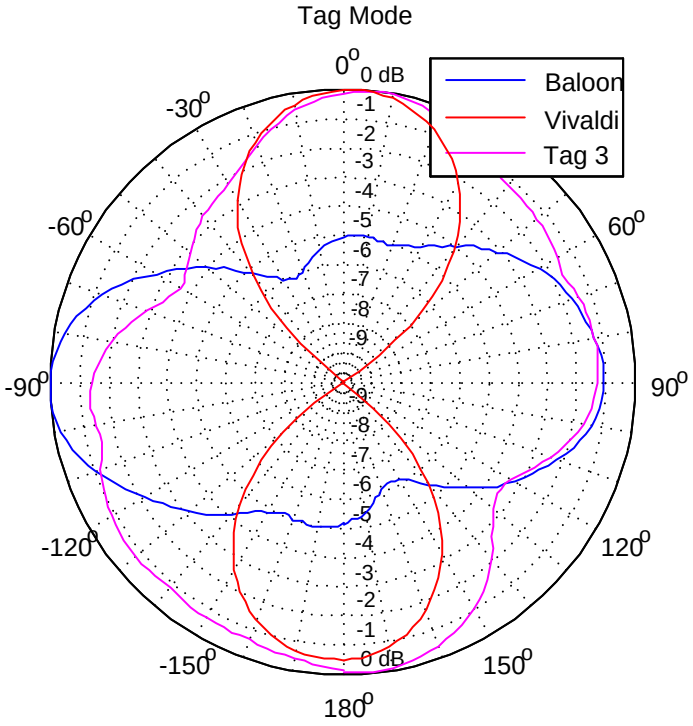

Figure 4.30. Normalized radiated power of the three antennas in all angles.

References

[1] David Girbau, Ángel Ramos, Antonio Lázaro, Sergi Rima, and Ramón Villarino, "Passive Wireless Temperature Sensor Based on Time-Coded UWB Chipless RFID Tags", "IEEE TRANSACTIONS ON MICROWAVE THEORY AND TECHNIQUES", 2012, Vol. 60, No. 11, pages 3623-3632.

5. Conclusions and Future Lines

In this project UWB-RFID technology has been studied and some chipless UWB-RFID tags have been designed and implemented; this has been interesting because it is an emerging technology which is being studied nowadays with good results.

Tag 1 had really good results, it is the only one integrated tag (at least in the known literature), with such a good circular polarization and it was readable up to 2 meters from the reader. Tag 2 was not as good as 1, simulations brought to mind that the polarization would be better in that case but in Chapter 4 it has been demonstrated that it did not work so good, although still offered good results for a chipless RFID tag. On the other hand Tag 3, had a too big structure which caused a structural mode which masked tag mode, but it wasn't until the delay line was cut, when right readings could be done, which probably means there was a conflict in the integration of the delay line.

Using Tag 1, many researches about delay-line based chipless UWB-RFID tags, can be improved because Tag 1 will allow better readings of the tag, no matter the direction of the tag, since using the antennas of the reader cross-polarized avoids coupling between them and using circularly-polarized antennas at the tag permits good read ranges at any tag orientation.

Apart from that, I really appreciate all the new knowledge I've acquired though this project, I have not only learned new concepts but I've also reinforced others that I had learned during my actual degree.